

UNLOCKING THE VALUE OF TEXT: EVENT-DRIVEN REASONING AND MULTI-LEVEL ALIGNMENT FOR TIME SERIES FORECASTING

Anonymous authors
Paper under double-blind review

ABSTRACT

Existing time series forecasting methods primarily rely on the numerical data itself. However, real-world time series exhibit complex patterns associated with multimodal information, making them difficult to predict with numerical data alone. While several multimodal time series forecasting methods have emerged, they either utilize text with limited supplementary information or focus merely on representation extraction, extracting minimal textual information for forecasting. To unlock the Value of Text, we propose VoT, a method with Event-driven Reasoning and Multi-level Alignment. Event-driven Reasoning combines the rich information in exogenous text with the powerful reasoning capabilities of LLMs for time series forecasting. To guide the LLMs in effective reasoning, we propose the Historical In-context Learning that retrieves and applies historical examples as in-context guidance. To maximize the utilization of text, we propose Multi-level Alignment. At the representation level, we utilize the Endogenous Text Alignment to integrate the endogenous text information with the time series. At the prediction level, we design the Adaptive Frequency Fusion to fuse the frequency components of event-driven prediction and numerical prediction to achieve complementary advantages. Experiments on real-world datasets across 10 domains demonstrate significant improvements over existing methods, validating the effectiveness of our approach in the utilization of text. The code is made available at <https://anonymous.4open.science/r/VoT-465C>.

1 INTRODUCTION

Time series forecasting is a fundamental task in numerous domains, including financial market analysis, climate monitoring, and healthcare management. Deep learning-based forecasting methods have achieved competitive performance (Nie et al., 2023; Liu et al., 2024b; Chang et al., 2025) on this task. However, they solely rely on numerical time series data, limiting their ability to capture more complex patterns.

Taking the unemployment rate data (Liu et al., 2024a) as an example, Figure 1 illustrates that certain abrupt changes in the time series are difficult to predict solely from historical numerical patterns. However, by incorporating textual information, the model may get crucial guidance that helps forecast sudden shifts, such as the unemployment rate spikes triggered by the 2008 financial crisis and the COVID-19 pandemic in 2020. This demonstrates that text serves as a valuable complementary modality, enriching time series forecasting with event-driven guidance that is not easily inferred from numerical data alone. Moreover, textual in-

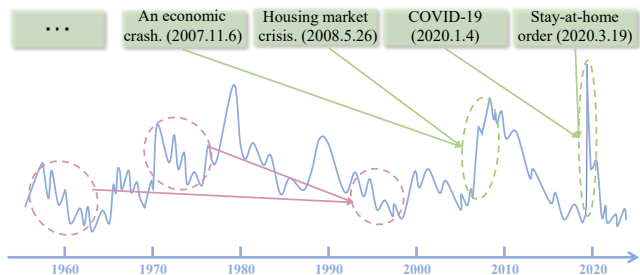


Figure 1: Unemployment rate time series (Liu et al., 2024a) (1970-2020). While certain patterns (pink) exhibit predictable temporal regularities, abrupt changes (green) driven by external events necessitate the integration of textual information to complement numerical forecasting.

formation predominantly contributes to capturing event-related dynamics, but lacks descriptions of subtle fluctuations. However, this missing information can be supplemented through time series modeling. By jointly leveraging these complementary strengths, the model can better integrate the forecasting abilities of the two modalities, thereby breaking the limitations of single modality.

To explore the potential of textual information and effectively apply it in time series forecasting, there exist two main challenges. **The first challenge** is insufficient text utilization. Some approaches incorporate prompts based on *endogenous text* (Kowsher et al., 2024), such as statistical summaries or dataset-specific descriptions. While this text offers useful context, it largely overlaps with information already present in the time series. Consequently, they are unable to effectively model external drivers of temporal dynamics. On the other hand, some methods (Luo et al., 2023; Zhang et al., 2024) leverage LLMs to embed *exogenous text* (Liu et al., 2024a), which has richer textual sources, such as news and policy documents. These methods primarily focus on the representation-level fusion and are difficult to explore the deep semantic information, leaving the potential value of textual information untapped. **The second challenge** is effectively aligning two modalities to leverage their complementary strengths. While text provides crucial guidance for sudden shifts and event-related dynamics, time series modeling captures the subtle fluctuations and numerical trends that text cannot describe. However, the considerable modality gap between these modalities prevents existing methods from achieving effective cross-modal integration.

Based on these insights, we propose VoT, a novel multimodal time series forecasting method that leverages Event-driven Reasoning and Multi-level Alignment to effectively unlock the value of textual information. Our approach employs a dual-branch architecture to integrate both exogenous and endogenous text for comprehensive time series forecasting. *Event-driven Reasoning* is performed through our Event-Driven Prediction Branch, which employs a generative pipeline that includes template generation, summarization, and reasoning. This pipeline enables LLMs to extract more forecasting-related information from exogenous text. Additionally, we introduce Historical In-Context Learning (HIC), which provides error-informed guidance from historical samples for reasoning. *Multi-level alignment* is designed to fully integrate the predictive capabilities of time series and text. At the representation level, we introduce the numerical prediction branch with an Endogenous Text Alignment (ETA). The ETA first converts temporal statistics into textual descriptions and then uses decomposed pattern extraction and decomposed contrastive learning to achieve alignment between two modalities. At the prediction level, we introduce the Adaptive Frequency Fusion (AFF) that dynamically adjusts importance and integrates the frequency components of outputs from the event-driven prediction branch and the numerical prediction branch. Based on dynamic frequency fusion, the AFF enables domain-driven optimization to achieve complementary advantages and address the varying dependencies on textual and numerical information across different datasets. Specifically, we make the following contributions:

- We introduce an event-driven reasoning method to extract the forecasting-related information from exogenous text and obtain numerical predictions. It is enhanced by Historical In-Context Learning (HIC), which retrieves historical reasoning examples as prompts to provide error-informed guidance for reasoning. The method improves the reasoning ability of LLMs and unlocks the value of text.
- We propose a multi-level alignment approach. Specifically, we introduce the Endogenous Text Alignment (ETA) for representation-level alignment and the Adaptive Frequency Fusion (AFF) for prediction-level alignment. Through comprehensive alignment, we achieve complementary advantages across both modalities.
- We conduct extensive experiments on 10 real-world datasets from different domains and achieve state-of-the-art prediction accuracy. Moreover, we conduct thorough ablation and analysis experiments to demonstrate our effective utilization of text.

2 RELATED WORK

Time Series Forecasting Time series forecasting has evolved from traditional statistical methods like exponential smoothing (Hyndman & Khandakar, 2008; Li et al., 2022a) to deep learning approaches. Deep learning methods have rapidly developed and can be broadly categorized into MLP-based (Zeng et al., 2023), RNN-based (Chung et al., 2014; Kieu et al., 2022; Wen et al., 2017; Cirstea et al., 2019), CNN-based (Sen et al., 2019; Liu et al., 2022; Wang et al., 2023), GNN-based

Table 1: Comparison of multimodal time series forecasting methods with text incorporation

	Sub-categories	Ours	GPT4TS (2025)	TimeLLM (2023b)	TEST (2024)	CALF (2025a)	CMIN (2023)	Maformer (2024)	DualTime (2024)	Time-MMD (2024a)	TaTS (2025)	FNSPID (2024)	GPT4MTS (2024)	CiK (2024)
LM Usage	Feature Extraction	✓	✓	✓	✓	✓	✓	✓	✓	✓	✓	✓	✓	✓
	Reasoning	✓	✗	✗	✗	✗	✗	✗	✗	✗	✗	✗	✗	✗
Text Type	Endogenous	✓	✓	✓	✓	✓	✗	✗	✗	✗	✗	✗	✗	✓
	Exogenous	✓	✗	✗	✗	✗	✓	✓	✓	✓	✓	✓	✓	✓

(Jin et al., 2023a; Cheng et al., 2024), and Transformer-based (Zhou et al., 2021; Nie et al., 2023; Liu et al., 2024b; 2025b) models. These models primarily focus on the time series modality.

Multimodal Time Series Forecasting with Text Incorporation. The potential of leveraging textual information through LLMs for time series prediction has been widely accepted. Some methods like GPT4TS (Chang et al., 2023), TimeLLM (Jin et al., 2023b), and TEST (Sun et al., 2024) focus on enabling LLMs to understand time series through various encoding approaches, while CALF (Liu et al., 2025a) aligns temporal and text token distributions, and TimeVLM (Zhong et al., 2025) extends to visual modalities. However, these approaches primarily rely on temporal information without extensive exogenous text utilization. In fields like finance and health with rich multimodal data, CMIN (Luo et al., 2023), Modality-aware Transformer (Emami-Gohari et al., 2024), DualTime(Zhang et al., 2024) et al. have started integrating exogenous texts and time series. MM-TSFLib(Liu et al., 2024a) then extended such text utilization to more fields by collecting time-aligned text-time series datasets across multiple domains. Building on this, TaTS (Li et al., 2025) discovered that time-aligned text and time series exhibit similar periodicity. FNSPID (Dong et al., 2024) and GPT4MTS (Jia et al., 2024) place greater emphasis on text processing, filtering and summarizing text to obtain effective textual information. CiK (Williams et al., 2024) proposes metrics for textual utility evaluation. As summarized in Table 1, existing methods either use LMs only for feature extraction or handle only one text type (endogenous or exogenous). In contrast, our method VoT is the first to jointly leverage LMs for both feature extraction and reasoning, while supporting both endogenous and exogenous text, enabling more comprehensive multimodal forecasting.

3 METHODOLOGY

3.1 PROBLEM FORMULATION

Consider a time series $\mathbf{X} = \{\mathbf{x}_1, \mathbf{x}_2, \dots, \mathbf{x}_L\} \in \mathbb{R}^{L \times N}$, where L denotes the length of the look-back window and N represents the number of variables. Each time point $\mathbf{x}_t \in \mathbb{R}^N$ is associated with textual information \mathbf{T}_t . As mentioned in the introduction, we divide textual information \mathbf{T}_t into two categories based on their source and characteristics.

Exogenous text \mathbf{T}^{ex} (Liu et al., 2024a) originates from external sources such as news articles, policy announcements, or social media posts, describing events, contexts, and factors that influence the time series beyond the system itself. **Endogenous text \mathbf{T}^{en}** (Kowsher et al., 2024) consists of structured textual descriptions derived directly from time series statistics.

The objective of multimodal time series forecasting is to predict the future H time steps $\mathbf{Y} = \{\mathbf{x}_{L+1}, \mathbf{x}_{L+2}, \dots, \mathbf{x}_{L+H}\} \in \mathbb{R}^{H \times N}$ by leveraging both historical observations and their associated textual information:

$$\hat{\mathbf{Y}} = \mathcal{F}(\mathbf{X}, \mathbf{T}^{\text{ex}}, \mathbf{T}^{\text{en}}, \theta) \quad (1)$$

where $\hat{\mathbf{Y}} \in \mathbb{R}^{H \times N}$ represents the predicted values, \mathcal{F} denotes the multimodal forecasting model, and θ encompasses all learnable parameters.

3.2 OVERVIEW

To maximize text utilization and enable mutual complementarity between textual and temporal information, we propose a dual-branch architecture that comprehensively leverages both exogenous and endogenous textual information. As illustrated in Figure 2, our method consists of two complementary branches that supports Event-driven Reasoning and Multi-level Alignment. The event-driven prediction branch primarily focuses on extracting predictive information from the exogenous text and the numerical prediction branch aligns time series with the generated endogenous text. For

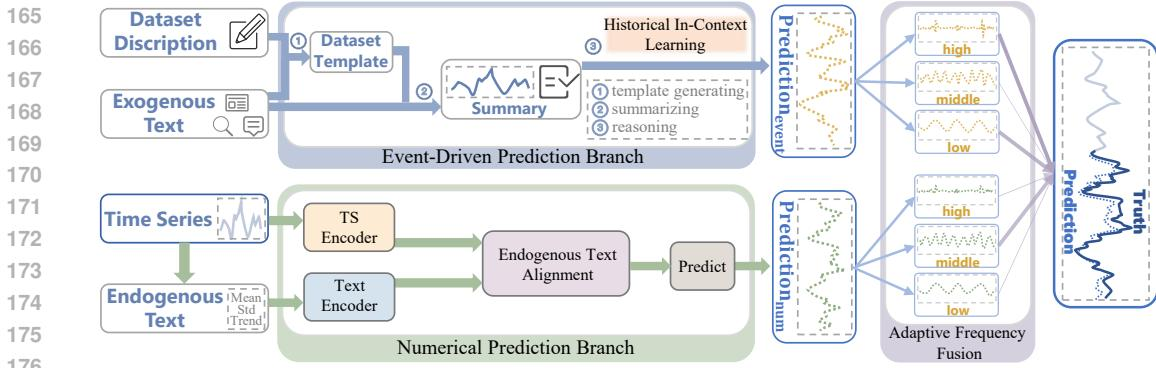


Figure 2: Overview of the proposed dual-branch multimodal forecasting framework. The event-driven branch processes exogenous text through a three-step generative pipeline with the Historical In-Context Learning (HIC). The numerical branch aligns endogenous text with time series via the Endogenous Text Alignment (ETA). The Adaptive Frequency Fusion (AFF) combines both predictions across frequency bands with adaptive weights.

Event-driven Reasoning, the event-driven prediction branch extracts contextual information from exogenous text through a three-step generative pipeline. The pipeline is powered by the Historical In-Context Learning (HIC). Multi-level Alignment is designed to fully integrate the predictive capabilities of two modalities. At the representation level, the numerical prediction branch employs an Endogenous Text Alignment (ETA) to extract textual features aligned with time series patterns. At the prediction level, we introduce Adaptive Frequency Fusion (AFF). It fuses the frequency components of event-driven prediction and numerical prediction. Rather than assuming fixed influence of exogenous text on time series, AFF learns optimal fusion strategies directly from the dataset through Fourier decomposition and learnable frequency-specific weights.

3.3 EVENT-DRIVEN REASONING

To strengthen the reasoning capabilities of LLMs for time series forecasting, we propose a three-step generative pipeline including template generation, summarization, and reasoning. It converts exogenous text into event-driven numerical predictions enriched with contextual information. Additionally, we propose the Historical In-Context Learning (HIC). It keeps historical reasoning samples during training and retrieves similar examples as error-informed guidance during inference, as shown in Figure 3. The retrieved examples are corrected to provide guidance that helps avoid similar errors. By integrating these examples, LLMs are enhanced to generate accurate and error-informed predictions.

3.3.1 GENERATIVE PIPELINE

To process exogenous text T^{ex} into numerical predictions, we implement a three-step generative pipeline. First, LM generates a dataset-specific template \mathcal{D} based on the dataset description and exogenous text-time series samples, which serves as a structured dictionary containing key-value mappings that guide the extraction of predictive information. Second, we use this template \mathcal{D} to generate summaries S_i from raw exogenous text T_i^{ex} and time series \mathbf{X}_i , filtering redundant information while preserving the information influential to time series forecasting. Finally, we employ the Reasoner, which is a reasoning model to process these summaries and generate predictions:

$$\hat{\mathbf{Y}}_i^{\text{event}}, \mathcal{R}_i = \text{Reasoner}(\mathcal{P}_{\text{reason}}, S_i, \mathbf{X}_i) \quad (2)$$

The reasoning model Reasoner generates both the numerical prediction $\hat{\mathbf{Y}}_i^{\text{event}} \in \mathbb{R}^{H \times N}$ and the explanatory reasoning process \mathcal{R}_i . $\mathcal{P}_{\text{reason}}$ is a carefully designed prompt that guides the LLM to perform structured reasoning from summaries S_i and time series \mathbf{X}_i to numerical predictions. However,

220 this basic pipeline operates in an unsupervised manner, which may introduce suboptimal guidance
 221 for numerical prediction patterns, potentially amplifying prediction errors. Accordingly, we design
 222 the Historical In-Context Learning (HIC) to solve the problem.
 223

224 **3.3.2 HISTORICAL IN-CONTEXT LEARNING**

226 To make the prediction more accurate, we introduce Historical In-Context Learning (HIC), which
 227 synergizes historical reasoning information with In-Context Learning (ICL), as shown in Figure 3.
 228 During training, it corrects the reasoning process with ground-truth and keeps the corrected samples.
 229 The optimized reasoning process of the corrected samples keeps information about why errors exist
 230 and correct reasoning strategies. During inference, it retrieves the most similar historical example
 231 and integrates it into the reasoning prompt to obtain error-informed guidance and accurately forecast.
 232

233 **Knowledge Base Construction.** During training, HIC builds a Knowledge Base \mathcal{K} by learning from
 234 prediction errors. As mentioned, the Reasoner generates initial predictions $\hat{\mathbf{Y}}_i^{\text{event}}$ and reasoning
 235 processes \mathcal{R}_i . After that, the Reasoner creates corrected reasoning \mathcal{C}_i using ground truth \mathbf{Y}_i :

$$\mathcal{C}_i = \text{Reasoner}(\mathcal{P}_{\text{correct}}, \hat{\mathbf{Y}}_i^{\text{event}}, \mathcal{R}_i, \mathbf{Y}_i, \mathbf{X}_i) \quad (3)$$

236 where $\mathcal{P}_{\text{correct}}$ is the prompt that guides the Reasoner to identify and understand what caused the
 237 error between the initial predictions $\hat{\mathbf{Y}}_i^{\text{event}}$ and the ground-truth \mathbf{Y}_i . Correction \mathcal{C}_i explains how
 238 to accurately derive the actual values given the context, and crucially, it contains analysis of the
 239 previous prediction errors, which helps Reasoner better understand and avoid similar errors in the
 240 future. The Knowledge Base \mathcal{K} stores pairs of summary embeddings of summaries $\{\mathcal{S}_i\}_{i=1}^M$ and
 241 their corresponding correction $\{\mathcal{C}_i\}_{i=1}^M$:

$$\mathcal{K} = \{(\text{Embed}(\mathcal{S}_i), \mathcal{C}_i)\}_{i=1}^M \quad (4)$$

242 where M denotes the number of training samples, Embed is an embedding model.
 243

244 **Retrieval-Guided Prediction.** During inference, HIC retrieves the most similar historical example
 245 from \mathcal{K} to obtain error-informed guidance for forecasting. Given a data pair $(\mathbf{X}_j, \mathbf{T}_j^{\text{ex}})$, first LM
 246 generates the summary \mathcal{S}_j . Then using the embedding of the summary \mathcal{S}_j , HIC retrieves the most
 247 similar example in the Knowledge Base:
 248

$$\tilde{i} = \arg \max_{(\mathcal{S}_i, \mathcal{C}_i) \in \mathcal{K}} \text{simi}(\text{Embed}(\mathcal{S}_j), \text{Embed}(\mathcal{S}_i)) \quad (5)$$

249 where simi is the similarity metric. The retrieved corresponding correction $\mathcal{C}_{\tilde{i}}$ serves as an in-context
 250 example, improving the reasoning accuracy with error-informed guidance:
 251

$$\hat{\mathbf{Y}}_j^{\text{event}} = \text{Reasoner}(\mathcal{P}_{\text{ICL}}, \mathcal{C}_{\tilde{i}}, \mathcal{S}_j, \mathbf{X}_j) \quad (6)$$

252 where \mathcal{P}_{ICL} is the prompt that combines the retrieved correction $\mathcal{C}_{\tilde{i}}$ as guidance for current inference.
 253

254 By retrieving historically corrected reasoning patterns, HIC provides error-informed guidance for
 255 LLMs. The error-informed learning helps the model understand how exogenous text impacts time
 256 series, thereby improving predictions when similar event-driven fluctuations occur. Moreover, HIC
 257 achieves this without requiring expensive fine-tuning, making it efficient and scalable across different
 258 forecasting domains.
 259

260 Event-driven Reasoning generates numerical predictions by leveraging semantic information in exogenous
 261 text and capturing event-driven dynamics. Through correcting the reasoning process, constructing a
 262 knowledge base, and implementing a retrieve-and-guide mechanism, our approach enhances the reasoning
 263 ability of LLM while maximizing text utilization.
 264

265 **3.4 MULTI-LEVEL ALIGNMENT**

266 While the event-driven prediction branch excels at capturing external influences through exogenous
 267 text, not all temporal variations are reflected in or captured by exogenous text. Some data follow
 268 intrinsic patterns that are better captured through numerical analysis. To fully leverage the advantages
 269 of both modalities, we design a Multi-level Alignment method. It performs representation-level
 270 alignment with endogenous text via the Endogenous Text Alignment (ETA) of the numerical branch.
 271 In the prediction level, it employs Adaptive Frequency Fusion (AFF) to align exogenous text prediction
 272 with numerical prediction and integrate results from both branches. The outputs obtained after
 273 deep alignment obtain the complementary advantages of both modalities.
 274

275 3.4.1 REPRESENTATION-LEVEL ALIGNMENT
276

277 To achieve representation-level alignment, the
278 numerical prediction branch employs an En-
279 doogenous Text Alignment (ETA), as shown in
280 Figure 4. This module establishes deep seman-
281 tic alignment between temporal patterns and
282 their textual representations using decomposed
283 pattern extraction and decomposed contrastive
284 learning. Considering that trend and seasonal-
285 ity are intrinsic properties of time series, ETA
286 similarly extracts corresponding textual re-
287 presentations to achieve fine-grained alignment be-
288 tween endogenous text and temporal patterns.

289 **Time Series and Text Encoding.** We encode
290 the input time series $\mathbf{X} \in \mathbb{R}^{L \times N}$ using an en-
291 coder to obtain temporal representations $\mathbf{H}^{\text{ts}} \in \mathbb{R}^{N \times d^{\text{ts}}}$. Simultaneously, we generate endogenous
292 text \mathbf{T}^{en} by converting statistical descriptors such as mean and frequency into structured textual
293 descriptions, which are then encoded using a LM to obtain text embeddings $\mathbf{H}^{\text{text}} \in \mathbb{R}^{L^{\text{text}} \times d^{\text{text}}}$,
294 where L and L^{text} denote the sequence length and text token length respectively, N is the number of
295 variables, and $d^{\text{ts}}, d^{\text{text}}$ are the embedding dimensions for time series and text respectively.

296 **Decomposed Pattern Extraction.** Our decomposed pattern extraction first employs the dual-query
297 attention to filter semantic components from text. First, we use learnable queries $\mathbf{Q}^{\text{tr}}, \mathbf{Q}^{\text{se}} \in \mathbb{R}^{N \times d^{\text{text}}}$
298 to extract trend and seasonal information $\mathbf{E}^{\text{tr}}, \mathbf{E}^{\text{se}} \in \mathbb{R}^{N \times d^{\text{text}}}$ related to time series from textual
299 representations:

$$300 \mathbf{E}^{\text{tr}} = \text{Attention}(\mathbf{Q}^{\text{tr}}, \mathbf{H}^{\text{text}}, \mathbf{H}^{\text{text}}), \quad \mathbf{E}^{\text{se}} = \text{Attention}(\mathbf{Q}^{\text{se}}, \mathbf{H}^{\text{text}}, \mathbf{H}^{\text{text}}) \quad (7)$$

302 Then, the ETA performs ts-text attention to align temporal representations with extracted textual
303 components, obtaining further aligned representations \mathbf{Z}^{tr} and \mathbf{Z}^{se} (cross-modal aligned features):

$$304 \mathbf{Z}^* = \text{Cross-Attention}(\text{Proj}(\mathbf{H}^{\text{ts}}), \mathbf{E}^*, \mathbf{E}^*), \quad * \in \{\text{tr}, \text{se}\} \quad (8)$$

306 where $\text{Proj}(\cdot) : \mathbb{R}^{d^{\text{ts}}} \rightarrow \mathbb{R}^{d^{\text{text}}}$ projects time series embeddings to the text embedding space, and
307 $\mathbf{Z}^{\text{tr}}, \mathbf{Z}^{\text{se}} \in \mathbb{R}^{N \times d^{\text{text}}}$ are the aligned trend and seasonal representations that combine information
308 from both modalities. To map these representations to the time series space for fusion, we apply:

$$309 \tilde{\mathbf{Z}}^* = \text{Proj}_{\text{inv}}(\mathbf{Z}^*), \quad * \in \{\text{tr}, \text{se}\} \quad (9)$$

311 where $\text{Proj}_{\text{inv}}(\cdot) : \mathbb{R}^{d^{\text{text}}} \rightarrow \mathbb{R}^{d^{\text{ts}}}$, yielding $\tilde{\mathbf{Z}}^{\text{tr}}, \tilde{\mathbf{Z}}^{\text{se}} \in \mathbb{R}^{N \times d^{\text{ts}}}$.

312 **Deep Semantic Alignment via Decomposed Contrastive Learning.** To achieve deep semantic
313 alignment between temporal patterns and textual representations, we employ contrastive learning
314 at the sample level. We first decompose the temporal representations \mathbf{H}_i^{ts} into trend and seasonal
315 components to obtain \mathbf{H}_i^{tr} and \mathbf{H}_i^{se} . Then, we get the mean representation $\bar{\mathbf{H}}_i^{\text{tr}}, \bar{\mathbf{H}}_i^{\text{se}} \in \mathbb{R}^{d^{\text{ts}}}$ and
316 $\bar{\mathbf{Z}}_i^{\text{tr}}, \bar{\mathbf{Z}}_i^{\text{se}} \in \mathbb{R}^{d^{\text{ts}}}$. We compute the contrastive loss for each component pair.

$$318 \mathcal{L}_{\text{align}} = \frac{1}{2} \sum (-\log \frac{\exp(\text{sim}(\bar{\mathbf{H}}_i^*, \bar{\mathbf{Z}}_i^*)))}{\sum_{j=1}^B \exp(\text{sim}(\bar{\mathbf{H}}_i^*, \bar{\mathbf{Z}}_j^*)))} - \log \frac{\exp(\text{sim}(\bar{\mathbf{Z}}_i^*, \bar{\mathbf{H}}_i^*)))}{\sum_{j=1}^B \exp(\text{sim}(\bar{\mathbf{Z}}_i^*, \bar{\mathbf{H}}_j^*)))}), \quad * \in \{\text{tr}, \text{se}\} \quad (10)$$

321 where $\text{sim}(\cdot, \cdot)$ denotes cosine similarity and B is the batch size. The total alignment loss combines
322 both trend and seasonal components. This objective ensures that corresponding trend and seasonal
323 components from both modalities are aligned in a shared representation space.

324 After completing the modal alignment, the numerical prediction output \mathbf{Y}_{num} is generated by fus-
325 ing temporal and text representations. Specifically, the calculation formula of \mathbf{Y}_{num} is defined as
326 $\mathbf{Y}_{\text{num}} = \frac{1}{2} \mathbf{H}^{\text{ts}} + \frac{1}{2} (\tilde{\mathbf{Z}}^{\text{tr}} + \tilde{\mathbf{Z}}^{\text{se}})$, where \mathbf{H}^{ts} represents the original temporal representation, and
327 $(\tilde{\mathbf{Z}}^{\text{tr}}, \tilde{\mathbf{Z}}^{\text{se}})$ denotes the text-derived representations corresponding to trend and seasonal components
328 respectively. The fusion process adopts equal weight allocation to balance the contributions of tem-
329 poral and textual information.

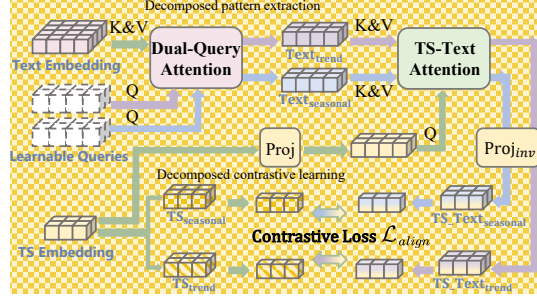


Figure 4: The processing procedure of the Endogenous Text Alignment (ETA).

330 3.4.2 PREDICTION-LEVEL ALIGNMENT
331

332 Event-driven predictions excel at capturing patterns influenced by external factors, while not all temporal
333 variations are reflected in or captured by textual information. These complementary strengths
334 can potentially be integrated through frequency-based approaches. Therefore, at the prediction level,
335 we introduce Adaptive Frequency Fusion (AFF) to dynamically adjust the importance of different
336 frequency components, thereby leveraging the complementary strengths of textual and numerical
337 information across frequency bands.

338 **Adaptive Frequency Fusion.** We decompose both branch predictions into frequency components:

$$339 \quad \mathcal{F}^{\text{num}} = \text{FFT}(\hat{\mathbf{Y}}^{\text{num}}), \quad \mathcal{F}^{\text{event}} = \text{FFT}(\hat{\mathbf{Y}}^{\text{event}}) \quad (11)$$

340 The spectrum is partitioned into three bands based on frequency. We extract band-specific components
341 with mask \mathbf{M} :

$$342 \quad \mathcal{F}_*^b = \mathcal{F}_* \odot \mathbf{M}^b, \quad * \in \{\text{num, event}\}, \quad b \in \{\text{low, mid, high}\} \quad (12)$$

343 Instead of using fixed fusion ratios, we introduce learnable weights $\mathbf{w} = w_*^b, * \in \{\text{num, event}\}, b \in$
344 $\{\text{low, mid, high}\}$ that adapt to data characteristics:

$$345 \quad \mathcal{F}_{\text{fused}} = \sum_* \sum_b w_*^b \mathcal{F}_*^b, * \in \{\text{num, event}\}, b \in \{\text{low, mid, high}\}, \quad \hat{\mathbf{Y}}_{\text{final}} = \text{iFFT}(\mathcal{F}_{\text{fused}}) \quad (13)$$

350 **Training Objective.** Our model is trained with a composite loss function:

$$353 \quad \mathcal{L}_{\text{total}} = \mathcal{L}_{\text{ts}} + \mathcal{L}_{\text{align}} + \mathcal{L}_{\text{final}} \quad (14)$$

354 where $\mathcal{L}_{\text{ts}} = \text{MSE}(\hat{\mathbf{Y}}_{\text{ts}}, \mathbf{Y})$ maintains base temporal prediction capability and $\hat{\mathbf{Y}}_{\text{ts}}$ is from the
355 numerical branch without ETA. $\mathcal{L}_{\text{align}}$ enforces cross-modal alignment via contrastive learning, and
356 $\mathcal{L}_{\text{final}} = \text{MSE}(\hat{\mathbf{Y}}_{\text{final}}, \mathbf{Y})$ optimizes the fused prediction accuracy.

358 4 EXPERIMENTS
359360 4.1 EXPERIMENTAL SETUP
361

363 **Datasets.** We evaluate VoT on 10 real-world multimodal time series datasets. 9 datasets are sourced
364 from the MM-TSFLib benchmark (Liu et al., 2024a), covering diverse domains including Agriculture,
365 Climate, Economy, Energy, Public Health (United States), Environment, Traffic, and Security.
366 Notably, the original Economy dataset in MM-TSFLib is arranged in reverse temporal order. We
367 reorder this dataset temporally to align with the natural progression of events and maintain temporal
368 consistency. Additionally, we introduce a new Weather dataset containing multimodal meteorological
369 observations. We follow the experimental settings from MM-TSFLib (Liu et al., 2024a) for
370 dataset preprocessing and forecasting configurations. Detailed dataset descriptions are provided in
371 the Appendix A.1. Notably, we do not apply the “Drop Last” trick to ensure a fair comparison
372 following the settings (Qiu et al., 2024).

373 **Baselines.** We compare VoT against eleven representative baselines: three time series-only methods
374 including iTransformer (Liu et al., 2024b), PatchTST (Nie et al., 2023), and RAFT (Han et al.,
375 2025); three text-enhanced variants iTransformer*, PatchTST*, and RAFT* that incorporate textual
376 information through the Time-MMD framework (Liu et al., 2024a); and five multimodal forecasting
377 methods including GPT4TS (Chang et al., 2023), GPT4MTS (Jia et al., 2024), TaTS (Li et al.,
378 2025), Time-VLM (Zhong et al., 2025) and CALF (Liu et al., 2025a). All baselines are imple-
379 mented using their official code repositories when available, with consistent experimental settings
380 and hyperparameter tuning on the validation set.

381 **Metrics.** We adopt two standard metrics in time series forecasting: Mean Squared Error (MSE)
382 and Mean Absolute Error (MAE). MSE emphasizes larger errors and is more sensitive to outliers,
383 while MAE provides a more interpretable measure of average prediction error. We report averaged
384 results across all prediction horizons for comprehensive evaluation in the 4.2, with detailed results
for individual horizons provided in the G.

385 Table 2: Forecasting results of time series-only, text-enhanced, and our methods. The best results
 386 are highlighted in **bold**, and the second-best results are underlined.

Category	Models	Time series-only						Text-enhanced							
		Ours		PatchTST (2023)		iTTransformer (2024b)		RaFT (2025)		PatchTST*		iTTransformer*		RaFT*	
Metric		MSE	MAE	MSE	MAE	MSE	MAE	MSE	MAE	MSE	MAE	MSE	MAE	MSE	MAE
Agriculture	0.209	0.302	0.228	0.303	<u>0.220</u>	0.308	0.226	0.322	0.232	0.316	0.229	0.310	0.246	0.333	
Climate	1.078	0.840	1.184	0.888	1.135	0.865	1.289	0.926	1.178	0.887	<u>1.117</u>	<u>0.858</u>	1.342	0.944	
Economy	0.201	0.353	<u>0.210</u>	<u>0.363</u>	0.222	0.378	0.265	0.411	0.219	0.370	0.213	0.367	0.275	0.420	
Energy	0.222	0.343	0.250	0.363	0.269	0.382	0.254	0.367	0.253	0.365	0.265	0.383	0.246	<u>0.360</u>	
Environment	0.268	0.380	0.317	0.395	<u>0.276</u>	<u>0.386</u>	0.339	0.423	0.318	0.397	0.278	0.390	0.337	0.422	
Health	1.205	0.714	1.432	0.804	1.519	0.833	1.833	0.975	<u>1.360</u>	<u>0.768</u>	1.713	0.915	1.788	0.963	
Security	70.117	3.937	<u>72.027</u>	<u>4.062</u>	75.042	4.217	77.204	4.473	<u>72.721</u>	4.177	74.032	4.154	76.587	4.448	
Social Good	0.804	0.389	0.944	0.475	0.961	0.463	0.968	0.484	<u>0.909</u>	0.427	1.027	0.515	0.970	0.477	
Traffic	0.169	0.232	0.176	<u>0.234</u>	0.184	0.238	0.288	0.382	<u>0.174</u>	0.239	0.184	0.237	0.300	0.394	
Weather	0.968	0.706	1.145	0.751	1.231	0.803	1.099	0.746	1.036	<u>0.707</u>	<u>1.004</u>	0.709	1.096	0.745	
1st counts		20		0		0		0		0		0		0	

397 Table 3: Forecasting results of multimodal methods and ours. The best results are highlighted in
 398 **bold**, and the second-best results are underlined.

Models	Ours	GPT4TS (2025)		GPT4MTS (2024)		TaTS (2025)		Time-VLM (2025)		CALF (2025a)		
		MSE	MAE	MSE	MAE	MSE	MAE	MSE	MAE	MSE	MAE	
Agriculture	0.209	0.302	0.220	0.294	0.225	0.298	<u>0.215</u>	0.301	0.238	0.303	0.250	0.315
Climate	1.078	0.840	1.184	0.891	1.182	0.889	<u>1.180</u>	<u>0.887</u>	1.195	0.899	1.286	0.922
Economy	0.201	0.353	0.217	0.371	0.208	0.363	<u>0.215</u>	0.368	0.229	0.384	0.207	<u>0.357</u>
Energy	0.222	0.343	0.260	0.376	0.262	0.380	0.255	0.368	0.260	0.374	0.244	<u>0.365</u>
Environment	0.268	0.380	0.322	0.393	0.323	0.400	<u>0.319</u>	0.396	0.320	0.398	0.325	0.387
Health	1.205	0.714	1.341	0.777	1.464	0.799	1.356	<u>0.767</u>	1.490	0.835	1.491	0.775
Security	70.117	3.937	<u>71.165</u>	<u>4.047</u>	71.487	4.068	72.406	<u>4.097</u>	73.731	4.182	76.376	4.300
Social Good	0.804	0.389	0.917	0.476	0.920	0.450	0.918	0.428	<u>0.869</u>	0.444	0.906	<u>0.401</u>
Traffic	0.169	0.232	0.206	0.266	0.203	0.261	<u>0.179</u>	<u>0.238</u>	0.217	0.320	0.222	0.293
Weather	0.968	0.706	1.048	<u>0.708</u>	<u>0.986</u>	0.711	1.037	0.706	1.061	0.717	1.098	0.714
1st counts		19		1		0		1		0		0

4.2 MAIN RESULTS

412 Tables 2 and 3 present the outcomes of our comprehensive evaluation across 10 real-world multi-
 413 modal time series datasets. Our method achieves the best performance on nearly all datasets, ranking
 414 first in all 20 metrics against time series-only and text-enhanced baselines, and 19 out of 20 metrics
 415 against multimodal methods. This dominant performance across diverse domains demonstrates
 416 the effectiveness of our Event-driven Reasoning and Multi-level Alignment approach in leveraging
 417 both exogenous and endogenous textual information. Notably, our method demonstrates superior
 418 performance across diverse domains, particularly excelling on datasets that are susceptible to event
 419 influence and rich in exogenous textual information, such as Energy and Social Good.

4.3 MODEL ANALYSIS

4.3.1 ABLATION STUDIES

424 To validate the effectiveness of each component in our model, we conduct ablation studies on the En-
 425 ergy and Social Good datasets. Table 4 presents the ablation results. The TS-only baseline achieves
 426 0.250/0.944 MSE on Energy/Social Good, demonstrating significant performance gaps compared
 427 to our full method (0.222/0.804). Removing ETA (w/o ETA) degrades performance to 0.241/0.840
 428 MSE, confirming that structured textual descriptions enhance pattern recognition. Without HIC (w/o
 429 HIC), performance drops to 0.238/0.845 MSE, with more significant degradation on Social Good,
 430 validating that the retrieve-and-guide mechanism is crucial for event-driven forecasting. Without
 431 it, the LLM cannot be effectively guided in its reasoning process. Notably, removing HIC results
 432 in worse performance than removing the entire event-driven branch (w/o Event), suggesting that
 433 unguided LLM reasoning can be more detrimental than no reasoning at all. When equipped with
 434 proper guidance, the event-driven branch becomes highly effective, as evidenced by the significant
 435 performance gap between our full model (0.222/0.804) and the w/o Event baseline (0.232/0.841).

4.3.2 TEXT ANALYSIS

436 To verify whether the event-driven branch of VoT truly captures semantic information from text to
 437 enhance time series forecasting, we conduct a text replacement experiment. Specifically, we compare

		Event	HIC	AFF					
	Num	ETA			TS-only	w/o ETA	w/o HIC	w/o Event	ours
Energy	MSE	0.250	0.241	0.238	0.243	0.222			
Energy	MAE	0.363	0.355	0.363	0.360	0.343			
Social Good	MSE	0.944	0.840	0.845	0.876	0.804			
Social Good	MAE	0.475	0.424	0.410	0.436	0.389			

Table 4: Ablation study results on Energy and Social Good datasets

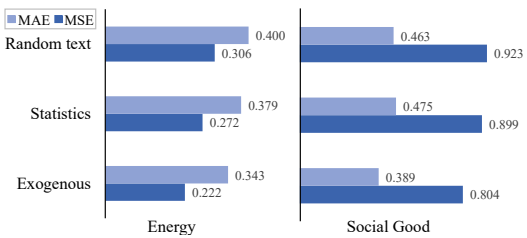


Figure 5: Ablation study on different text sources for event-driven reasoning.

our approach using exogenous text with two alternatives: randomly generated text and statistics-based text derived from the time series. As shown in Figure 5, results clearly demonstrate the superiority of exogenous text across both datasets. On the Energy dataset, exogenous text achieves 27.5% lower MSE and 14.3% lower MAE compared to random text. Similar improvements are observed on the Social Good dataset with 12.8% MSE reduction and 16.0% MAE reduction. The statistics show intermediate performance, suggesting that while time series-derived features provide some value, they cannot match the rich contextual information from real-world exogenous sources. This confirms that it is of great significance for us to propose an event-driven prediction branch and incorporate exogenous texts into the multimodal time series forecasting methods.

4.3.3 ADAPTIVE FREQUENCY FUSION ANALYSIS

To further validate the necessity of the AFF, we conduct frequency-domain analysis on the Social Good dataset, as shown in Figure 6. We apply different frequency filters to analyze the frequency characteristics of each branch. In Figure 6 (b), the low-pass filtered signals (0-10% frequencies), the event-driven branch aligns more closely with the ground truth than the TS-only branch, demonstrating its strength in capturing trend patterns and event-induced shifts; In Figure 6 (c), the high-pass filtered signals (70-100% frequencies), the TS-only method better matches the ground truth, effectively capturing short-term fluctuations and periodic patterns; In Figure 6 (d), the band-pass filtered signals (10-70% frequencies) reveal increased similarity among all methods, indicating dissimilarity is much more prevalent in high and low frequencies. These observations empirically confirm that different prediction branches excel in distinct frequency bands, highlighting the need for frequency fusion methods. Since different datasets exhibit varying degrees of correlation with events, resulting in different frequency component distributions, adaptive fusion is necessary. This validates the necessity and effectiveness of our AFF over fixed combination strategies.

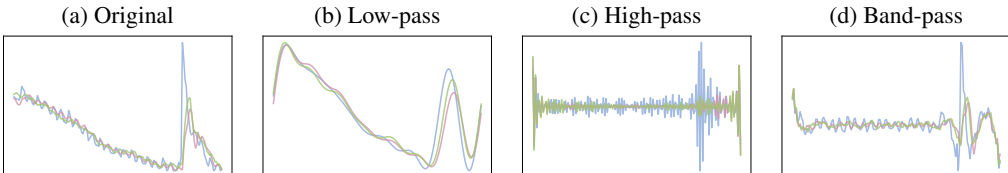


Figure 6: Frequency domain analysis of time series predictions (Social Good). (a)Original signals comparing ground truth. (b)-(d) Frequency-filtered components: (b) Low-pass filtered signals, (c) High-pass filtered signals, and (d) Band-pass filtered signals. Ground Truth (blue), Time series-only prediction (pink), and event-driven prediction (green)

5 CONCLUSION

In this paper, we presented VoT, a multimodal time series forecasting method that unlocks the value of textual information through Event-driven Reasoning and Multi-level Alignment. Our approach leverages both exogenous and endogenous text via a dual-branch architecture, where Historical In-Context Learning enables LLMs to learn from historical prediction errors, Endogenous Text Alignment bridges the semantic gap between modalities, and Adaptive Frequency Fusion dynamically combines their complementary strengths. Extensive experiments across 10 real-world datasets demonstrate that VoT achieves state-of-the-art performance, particularly excelling on event-influenced domains. Our work establishes that textual information provides irreplaceable contextual guidance for time series forecasting, and that effectively integrating these textual contexts with numerical patterns is crucial for advancing beyond the limitations of single-modality approaches.

495 ETHICS STATEMENT

496

497 Our work exclusively uses publicly available benchmark datasets that contain no personally identifiable information. The proposed anomaly detection framework is designed for beneficial applications

498 in system reliability and safety monitoring. No human subjects were involved in this research.

499

500 REPRODUCIBILITY STATEMENT

501

502 To ensure reproducibility, we provide: (1) Complete implementation details in Appendix A.4; (2)

503 Source code and scripts are provided in an anonymous repository at [<https://anonymous.4open.science/r/VoT-465C>]; (3) Fixed random seeds for all stochastic components.

504

505 ACKNOWLEDGMENTS

506 REFERENCES

507 Ching Chang, Wen-Chih Peng, and Tien-Fu Chen. Llm4ts: Two-stage fine-tuning for time-series

508 forecasting with pre-trained llms. *CoRR*, 2023.

509

510 Ching Chang, Wei-Yao Wang, Wen-Chih Peng, and Tien-Fu Chen. LLM4TS: aligning pre-trained

511 llms as data-efficient time-series forecasters. *ACM Trans. Intell. Syst. Technol.*, 16(3):60:1–60:20,

512 2025. doi: 10.1145/3719207. URL <https://doi.org/10.1145/3719207>.

513

514 Yunyao Cheng, Peng Chen, Chenjuan Guo, Kai Zhao, Qingsong Wen, Bin Yang, and Christian S.

515 Jensen. Weakly guided adaptation for robust time series forecasting. *Proceedings of the VLDB*

516 *Endowment*, 2024.

517 Junyoung Chung, Çağlar Gülcöhre, KyungHyun Cho, and Yoshua Bengio. Empirical evaluation of

518 gated recurrent neural networks on sequence modeling. *CoRR*, 2014.

519

520 Razvan-Gabriel Cirstea, Bin Yang, and Chenjuan Guo. Graph attention recurrent neural networks

521 for correlated time series forecasting. In *International Conference on Knowledge Discovery &*

522 *Data Mining (KDD)*, 2019.

523

524 Zihan Dong, Xinyu Fan, and Zhiyuan Peng. FNSPID: A comprehensive financial news dataset in

525 time series. In Ricardo Baeza-Yates and Francesco Bonchi (eds.), *Knowledge Discovery and Data*

526 *Mining (KDD)*, 2024.

527 Hajar Emami-Gohari, Xuan-Hong Dang, Syed Yousaf Shah, and Petros Zerfos. Modality-aware

528 transformer for financial time series forecasting. In *International Conference on AI in Finance*

529 (*ICAF*), 2024.

530

531 Sungwon Han, Seungeon Lee, Meeyoung Cha, Sercan Ö. Arik, and Jinsung Yoon. Retrieval aug-

532 mented time series forecasting. *CoRR*, abs/2505.04163, 2025. doi: 10.48550/ARXIV.2505.

533 04163. URL <https://doi.org/10.48550/arXiv.2505.04163>.

534 Rob J Hyndman and Yeasmin Khandakar. Automatic time series forecasting: the forecast package

535 for r. *Journal of statistical software*, 2008.

536

537 Furong Jia, Kevin Wang, Yixiang Zheng, Defu Cao, and Yan Liu. GPT4MTS: prompt-based large

538 language model for multimodal time-series forecasting. In *Educational Advances in Artificial*

539 *Intelligence, (EAAI)*, 2024.

540 Ming Jin, Huan Yee Koh, Qingsong Wen, Daniele Zambon, Cesare Alippi, Geoffrey I Webb, Irwin

541 King, and Shirui Pan. A survey on graph neural networks for time series: Forecasting, classifica-

542 tion, imputation, and anomaly detection. *arXiv*, 2023a.

543

544 Ming Jin, Shiyu Wang, Lintao Ma, Zhixuan Chu, James Y. Zhang, Xiaoming Shi, Pin-Yu Chen,

545 Yuxuan Liang, Yuan-Fang Li, Shirui Pan, and Qingsong Wen. Time-llm: Time series forecasting

546 by reprogramming large language models. *CoRR*, 2023b.

550 Tung Kieu, Bin Yang, Chenjuan Guo, Razvan-Gabriel Cirstea, Yan Zhao, Yale Song, and Christian S.
 551 Jensen. Anomaly detection in time series with robust variational quasi-recurrent autoencoders. In
 552 IEEE International Conference on Data Engineering (ICDE), 2022.

553

554 Md. Kowsler, Md. Shohanur Islam Sobuj, Nusrat Jahan Prottasha, E. Alejandro Alanis,
 555 Özlem Özmen Garibay, and Niloofar Yousefi. Llm-mixer: Multiscale mixing in llms for time
 556 series forecasting. CoRR, abs/2410.11674, 2024. doi: 10.48550/ARXIV.2410.11674. URL
 557 <https://doi.org/10.48550/arXiv.2410.11674>.

558 Hao Li, Jie Shao, Kewen Liao, and Mingjian Tang. Do simpler statistical methods perform better in
 559 multivariate long sequence time-series forecasting? In International Conference on Information
 560 & Knowledge Management (CIKM), 2022a.

561

562 Zihao Li, Xiao Lin, Zhining Liu, Jiaru Zou, Ziwei Wu, Lecheng Zheng, Dongqi Fu, Yada Zhu,
 563 Hendrik F. Hamann, Hanghang Tong, and Jingrui He. Language in the flow of time: Time-series-
 564 paired texts weaved into a unified temporal narrative. CoRR, 2025.

565

566 Haoxin Liu, Shangqing Xu, Zhiyuan Zhao, Lingkai Kong, Harshavardhan Kamarthi, Aditya B. Sasa-
 567 nur, Megha Sharma, Jiaming Cui, Qingsong Wen, Chao Zhang, and B. Aditya Prakash. Time-
 568 mmd: Multi-domain multimodal dataset for time series analysis. In Amir Globersons, Lester
 569 Mackey, Danielle Belgrave, Angela Fan, Ulrich Paquet, Jakub M. Tomczak, and Cheng Zhang
 (eds.), Neural Information Processing Systems (NeurIPS), 2024a.

570

571 Minhao Liu, Ailing Zeng, Muxi Chen, Zhijian Xu, Qiuxia Lai, Lingna Ma, and Qiang Xu. Scinet:
 572 Time series modeling and forecasting with sample convolution and interaction. In Advances in
 573 Neural Information Processing Systems (NeurIPS), 2022.

574

575 Peiyuan Liu, Hang Guo, Tao Dai, Naiqi Li, Jigang Bao, Xudong Ren, Yong Jiang, and Shu-Tao
 576 Xia. CALF: aligning llms for time series forecasting via cross-modal fine-tuning. In Toby
 577 Walsh, Julie Shah, and Zico Kolter (eds.), AAAI-25, Sponsored by the Association for the
 578 Advancement of Artificial Intelligence, February 25 - March 4, 2025, Philadelphia, PA, USA,
 579 pp. 18915–18923. AAAI Press, 2025a. doi: 10.1609/AAAI.V39I18.34082. URL <https://doi.org/10.1609/aaai.v39i18.34082>.

580

581 Yong Liu, Tengge Hu, Haoran Zhang, Haixu Wu, Shiyu Wang, Lintao Ma, and Mingsheng
 582 Long. itransformer: Inverted transformers are effective for time series forecasting. In The
 583 Twelfth International Conference on Learning Representations, ICLR 2024, Vienna, Austria,
 584 May 7-11, 2024. OpenReview.net, 2024b. URL <https://openreview.net/forum?id=JePfAI8fah>.

585

586 Yong Liu, Guo Qin, Xiangdong Huang, Jianmin Wang, and Mingsheng Long. Timer-xl: Long-
 587 context transformers for unified time series forecasting. In The Thirteenth International
 588 Conference on Learning Representations, ICLR 2025, Singapore, April 24-28, 2025. OpenRe-
 589 view.net, 2025b. URL <https://openreview.net/forum?id=KMCJXj1DDr>.

590

591 Di Luo, Weiheng Liao, Shuqi Li, Xin Cheng, and Rui Yan. Causality-guided multi-memory interac-
 592 tion network for multivariate stock price movement prediction. In Association for Computational
Linguistics (ACL), 2023.

593

594 Yuqi Nie, Nam H. Nguyen, Phanwadee Sinthong, and Jayant Kalagnanam. A time series is worth
 595 64 words: Long-term forecasting with transformers. In International Conference on Learning
Representations (ICLR), 2023.

596

597 Xiangfei Qiu, Jilin Hu, Lekui Zhou, Xingjian Wu, Junyang Du, Buang Zhang, Chenjuan Guo, Aoy-
 598 ing Zhou, Christian S. Jensen, Zhenli Sheng, and Bin Yang. TFB: towards comprehensive and
 599 fair benchmarking of time series forecasting methods. Proc. VLDB Endow., 17(9):2363–2377,
 600 2024. doi: 10.14778/3665844.3665863. URL <https://www.vldb.org/pvldb/vol17/p2363-hu.pdf>.

602

603 Rajat Sen, Hsiang-Fu Yu, and Inderjit S. Dhillon. Think globally, act locally: A deep neural net-
 604 work approach to high-dimensional time series forecasting. In Advances in Neural Information
Processing Systems (NeurIPS), 2019.

605 Chenxi Sun, Hongyan Li, Yaliang Li, and Shenda Hong. TEST: text prototype aligned embedding
 606 to activate llm's ability for time series. In International Conference on Learning Representations,
 607 (ICLR), 2024.

608 Huiqiang Wang, Jian Peng, Feihu Huang, Jince Wang, Junhui Chen, and Yifei Xiao. MICN:
 609 multi-scale local and global context modeling for long-term series forecasting. In International
 610 Conference on Learning Representations (ICLR), 2023.

611 Ruofeng Wen, Kari Torkkola, Balakrishnan Narayanaswamy, and Dhruv Madeka. A multi-horizon
 612 quantile recurrent forecaster. arXiv, 2017.

613 Andrew Robert Williams, Arjun Ashok, Étienne Marcotte, Valentina Zantedeschi, Jithendaraa Sub-
 614 ramanian, Roland Riachi, James Requeima, Alexandre Lacoste, Irina Rish, Nicolas Chapados,
 615 and Alexandre Drouin. Context is key: A benchmark for forecasting with essential textual infor-
 616 mation. CoRR, 2024.

617 Ailing Zeng, Muxi Chen, Lei Zhang, and Qiang Xu. Are transformers effective for time series
 618 forecasting? In Association for the Advancement of Artificial Intelligence (AAAI), 2023.

619 Weiqi Zhang, Jiebiao Ye, Ziyue Li, Jia Li, and Fugee Tsung. Dualtime: A dual-adapter multimodal
 620 language model for time series representation. CoRR, 2024.

621 Siru Zhong, Weilin Ruan, Ming Jin, Huan Li, Qingsong Wen, and Yuxuan Liang. Time-vlm:
 622 Exploring multimodal vision-language models for augmented time series forecasting. CoRR,
 623 abs/2502.04395, 2025. doi: 10.48550/ARXIV.2502.04395. URL <https://doi.org/10.48550/arXiv.2502.04395>.

624 Haoyi Zhou, Shanghang Zhang, Jieqi Peng, Shuai Zhang, Jianxin Li, Hui Xiong, and Wancai Zhang.
 625 Informer: Beyond efficient transformer for long sequence time-series forecasting. In Association
 626 for the Advancement of Artificial Intelligence (AAAI), 2021.

631

632

633

634

635

636

637

638

639

640

641

642

643

644

645

646

647

648

649

650

651

652

653

654

655

656

657

658

659

660 A EXPERIMENTAL DETAILS
661662 A.1 DATASETS
663664 Our experiments utilize 10 multimodal time series datasets from two sources: **MM-TSFLib**
665 **Datasets (Liu et al., 2024a):** We adopt 9 datasets from the MM-TSFLib benchmark, maintaining
666 their original preprocessing and alignment procedures. These datasets span:
667668

- **Agriculture:** USDA broiler market prices with weekly market reports
- **Climate:** NOAA drought indices with monthly climate reports
- **Economy:** US international trade balance (chronologically reordered for our experiments)
- **Energy:** Weekly US gasoline prices from EIA
- **Health:** CDC influenza-like illness statistics
- **Environment:** New York EPA air quality measurements
- **Traffic:** FHWA vehicle miles traveled statistics
- **Security:** FEMA disaster declarations

669670 **Weather Dataset:** We introduce a new multimodal dataset containing hourly observations of
671 weather. Each data point includes four numeric variables (MINTEMP, MAXTEMP, HUMIDITY,
672 MAXHUMIDITY(OT)) aligned with natural language weather descriptions. The OT variable
673 represents the maximum humidity in local regions.
674675 We follow the experimental settings from MM-TSFLib (Liu et al., 2024a), with configurations varying
676 based on data reporting frequency:
677678 For Environment and Weather datasets, we use a lookback window of $L = 96$ time steps, with
679 forecasting horizons $H \in \{48, 96, 192, 336\}$ and a label window size of 48 for the decoder.
680681 For Health and Energy datasets, the lookback window is set to $L = 36$, with forecasting horizons
682 $H \in \{12, 24, 36, 48\}$ and a label window size of 18.
683684 For Agriculture, Climate, Economy, Security, Social Good, and Traffic datasets, we employ a look-
685 back window of $L = 8$, forecasting horizons $H \in \{6, 8, 10, 12\}$, and a label window size of 4.
686687 A.2 DATASET SPLIT AND TIME LEAKAGE MITIGATION
688689 Our dataset split is time-based. The first 70% of the data in temporal order serves as the training set,
690 the 70%-80% segment serves as the validation set, and the latest 20% serves as the test set. There is
691 no temporal overlap between the training, validation, and test sets. When constructing the knowledge
692 base, we exclusively use relevant data from the training set. During the inference phase, that is, when
693 the input is from the validation or test set, retrieving examples from the knowledge database only
694 returns training-set data. All these data are temporally prior to the data in the validation and test sets,
695 so no time leakage occurs.
696705 A.3 BASELINES
706707 We evaluate our approach against nine representative baselines spanning from pure time series meth-
708 ods to multimodal forecasting approaches. The baselines are selected based on their state-of-the-art
709 performance and represent diverse architectural designs from recent years. The specific code repos-
710 itories for each model are shown in Table 5711 For the text-enhanced variants (marked with *), we integrate textual information following the Time-
712 MMD framework implementation, which concatenates text embeddings with time series representa-
713 tions before the prediction layer. All models are evaluated under identical experimental conditions
714 with consistent data preprocessing and hyperparameter tuning protocols.

715 Table 5: Implementation details and code repositories for baseline methods
716

717 Category	718 Method	719 Repository
720 Time Series Only	iTransformer	https://github.com/thuml/iTransformer
	PatchTST	https://github.com/yuqinie98/PatchTST
	RAFT	https://github.com/archon159/RAFT
721 Text-Enhanced (Time-MMD)	iTransformer*	Based on iTransformer with Time-MMD text integration
	PatchTST*	Based on PatchTST with Time-MMD text integration
	RAFT*	Based on RAFT with Time-MMD text integration
	Time-MMD	https://github.com/AdityaLab/MM-TSlib
724 Multimodal Forecasting	GPT4TS	https://github.com/blacksnail789521/LLM4TS
	GPT4MTS	https://github.com/Flora-jia-jfr/GPT4MTS-Prompt-based-Large-Language-Model-for-Multimodal-timeseries-Forecasting
	TaTS	https://github.com/iDEA-iSAIL-Lab-UIUC/TaTS
	TimeVLM	https://github.com/CityMind-Lab/ICML25-TimeVLM
	CALF	https://github.com/Hank0626/CALF

729
730 **A.4 DETAILED IMPLEMENTATION SETTINGS**731
732 **Software Environment.** Our implementation uses PyTorch 2.5.0+cu121 with Python 3.10. All
733 experiments are conducted on Ubuntu 20.04 with CUDA 12.1.734 **Event-Driven Branch Configuration.**735

- 736 **Template Generation and Summarization:** We employ Ollama-wrapped Meta-Llama-3-
737 8B-Instruct for generating dataset-specific templates and extracting event summaries from
738 exogenous text.
- 739 **Knowledge Base Construction:** Historical patterns are embedded using Qwen2-
740 Embedding-0.6B (768-dimensional vectors) for efficient similarity retrieval.
- 741 **Reasoning and Optimization:** During inference, we utilize the DeepSeek API for gener-
742 ating predictions and performing reasoning correction. The most similar historical patterns
743 is retrieved based on cosine similarity.

744 **Numerical Branch Configuration.**745

- 746 **Backbone Architecture:** PatchTST with 2-layer encoder (e.layers=2).
- 747 **Endogenous Text Generation:** GPT-2 converts structured textual descriptions into repre-
748 sentation.

749 **Adaptive Frequency Fusion Settings.**750

- 751 **Band Partition:** Initial partition uses Low (0-10%), Mid (10-70%), High (70-100%) fre-
752 quency bands. The actual boundaries are adaptively adjusted based on the frequency spec-
753 trum characteristics of each dataset to ensure effective separation between Low, Mid, and
754 High components.

755
756 We conducted tests under different boundary conditions to evaluate the sensitivity of the
757 model and presented the results in Figure 7 of the updated version. The figure displays a
758 heat map of MSE or MAE values with respect to different low- and high-frequency bound-
759 aries. Through analysis of the results, we observe that with the change of low and high
760 frequency bounds, the results do not change significantly when the boundary selection is
761 reasonable, which means low sensitivity.762

- 763 **Weight Initialization:** All six fusion weights $w = [0.5, 0.5, 0.5, 0.5, 0.5, 0.5]$ for balanced
764 initial contributions from both branches across all frequency bands.

765 **Multi-Stage Training Protocol.**766

- 767 **Stage 1 (Pre-training):** Train PatchTST backbone for 10 epochs with MSE loss, learning
768 rate 1e-4, cosine annealing scheduler.
- 769 **Stage 2 (Alignment):** Train alignment module for 10 epochs with contrastive loss, learning
770 rate 1e-3, encoder weights frozen.

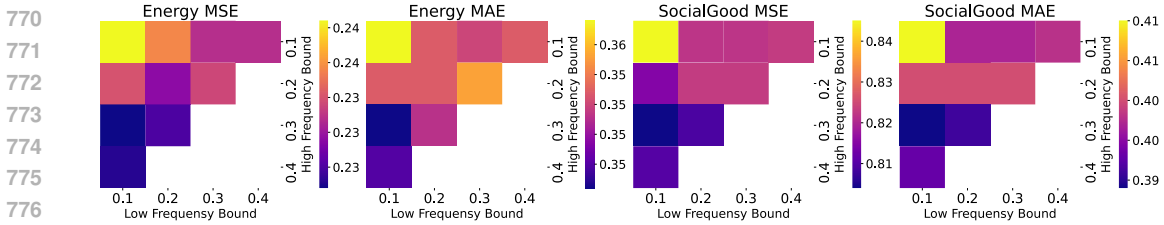


Figure 7: Heat Map of MSE/MAE Values Based on Low-Frequency and High-Frequency Percentage Cutoffs. The x-axis represents the percentage cutoffs for the low-frequency range, varying from 10% to 40% of the low-frequency spectrum. The y-axis represents the percentage cutoffs for the high-frequency range, ranging from 10% to 40% of the high-frequency spectrum. The color intensity in the map indicates the magnitude of the Mean Squared Error (MSE) or Mean Absolute Error (MAE)

- **Stage 3 (Joint Optimization):** Fine-tune all components for 30 epochs, learning rate selected from $\{5e-4, 1e-5\}$ based on validation performance.

Code Availability. The code is made available at <https://anonymous.4open.science/r/VoT-465C>.

A.5 EFFCIENCY ANALYSIS

As shown in the Table 6, the total latency is about 5.9s, which is mainly due to the Event-driven branch. LLM indeed brings additional cost. However, text analysis can bring abundant and valuable information which can help break the bottleneck of time series forecasting. That's why we need to investigate multimodal and additional cost brought by LLM is inevitable. But in most domains where multimodal is needed, the data is always sampled at a low frequency due to the fact that the collection of text needs time. And the time gap is enough for us to do the next value prediction. Therefore, second-level latency is acceptable. And when there is a high demand for real-time performance, we can use only the numerical branch, which is much faster and also effective.

Table 6: Inference Latency of Main Model Components

Branch / Module	Inference Time (s)
Event-driven Branch	5.9
Numerical Branch	0.002
AFF	0.0005

B HISTORICAL IN-CONTEXT LEARNING DESIGN DESCRIPTION

B.1 THE ABLATION OF HIC

We compare our HIC method with simpler retrieval-based approaches and presented the results in the Table 7. In the Table 7, "No Retrieval" represents the baseline case where no retrieval mechanism is used. "Retrieve TS" refers to the time series retrieval method, where the retrieval score is calculated as the cosine similarity between time series and the recalled data is time series. "Retrieve Summary" is the summary-based retrieval method, comparing the summary embedding similarity and recalling the summary. "Full HIC" indicates our complete HIC method.

As the results show, for the Climate dataset, the time series retrieval method slightly outperforms the "No Retrieval" baseline, but the improvement is marginal. On the SocialGood dataset, the time series retrieval method even leads to a performance degradation compared to the "No Retrieval" baseline. The summary-based retrieval method shows a more significant improvement over the time series retrieval method in terms of performance metrics. However, our complete HIC method achieves

the best performance, which indicates that the performance improvement is robust and primarily attributed to the full HIC module.

Table 7: Ablation Comparison of HIC with Simplified Retrieval Methods

Dataset	Method	MSE	MAE
Climate	No Retrieval	1.151	0.877
	Retrieve TS Only	1.137	0.866
	Retrieve Summary Only	1.091	0.846
	Full HIC	1.078	0.840
SocialGood	No Retrieval	0.845	0.410
	Retrieve TS Only	0.853	0.421
	Retrieve Summary Only	0.822	0.395
	Full HIC	0.804	0.389

B.2 ROBUSTNESS OF HIC WHEN RETRIEVING WITH LOW SIMILARITY

We conducted supplementary experiments to compare the results under different scenarios of similar example selection. Specifically, we retrieved the 10th - most similar and 100th - most similar examples to simulate the scenario where there are no close historical examples. The results are shown in the following Table 8

From these results, it can be observed that as the retrieval range of similar examples changes (from the 1st-most to the 100th-most similar example), and in comparison with the no-retrieval case (equivalent to disabling some functions of the HIC module), although the model performance fluctuates, it generally remains relatively stable. This further demonstrates the effectiveness and robustness of our design under different conditions.

Table 8: Model Robustness to Imperfect Retrieved Examples

Dataset	Retrieved Example by Similarity Rank	MSE	MAE
Energy	1st-most Similar Example	0.222	0.343
	10th-most Similar Example	0.229	0.348
	100th-most Similar Example	0.233	0.348
	No Retrieval	0.238	0.363
SocialGood	1st-most Similar Example	0.804	0.389
	10th-most Similar Example	0.807	0.408
	100th-most Similar Example	0.833	0.434
	No Retrieval	0.865	0.410

B.3 ROBUSTNESS TO NOISY/SPARSE TEXT DATA

We manually created relevant datasets. In our experiments, we introduced two types of modifications to simulate different real-world scenarios. For the sparse scenarios, we applied 10% and 20% masking to the text in the datasets. This included both discrete point masking (mask the text \mathbf{T}_i^{ex}) and continuous point masking (mask $\{\mathbf{T}_i^{ex}, \mathbf{T}_{i+1}^{ex}, \dots\}$). To simulate noisy scenarios, we added 10% and 20 noise to the text data. The experimental results, presented in the Table 9, show that while the performance does decrease slightly, the decline is not substantial. Moreover, our method still outperforms single-branch methods. These results demonstrate the robustness of our approach to noisy or sparse exogenous text. However, in extreme cases where all data is noisy or there is no valid text information available, the decline may be significant. In practice, severely degraded text data can be flagged via quality checks, mitigating negative impacts.

Table 9: Robustness Test of the Model Against Noisy and Sparse Text Data

Dataset	Condition	MSE	MAE
Climate	Mask 10% (mask10)	1.099	0.850
	Mask 20% (mask20)	1.109	0.854
	Noise 10% (noise10)	1.098	0.850
	Noise 20% (noise20)	1.103	0.854
	Our Method (Original)	1.078	0.840
SocialGood	Mask 10% (mask10)	0.822	0.448
	Mask 20% (mask20)	0.854	0.451
	Noise 10% (noise10)	0.836	0.412
	Noise 20% (noise20)	0.876	0.480
	Our Method (Original)	0.804	0.389

C ENDOGENOUS TEXT ALIGNMENT DESIGN DESCRIPTION

C.1 ENDOGENOUS TEXT ALIGNMENT ABLATION

The reason for adopting this method is that decomposition is a simple and widely-used technique in time series analysis. By decomposing the time series into trend and seasonal components, we can enrich the semantic representation of the time series to a certain degree. This enrichment allows for better alignment with textual information, facilitating more effective multi-modal interaction. To further validate the effectiveness of this approach, we conducted supplementary ablation experiments on the numerical branch. The "w/o decomposition" condition indicates the absence of trend and seasonal decomposition, with only standard TS-Text contrastive learning being performed. The "w/o TS-Text CL" condition means that only time series decomposition is applied, without TS-Text contrastive learning. The experimental results, as presented in Table 10, demonstrate that our proposed method, ETA, achieves superior performance compared to alternative designs.

Table 10: Ablation Study on Components of the Event-based Temporal Alignment (ETA)

Dataset	Fusion Method	MSE	MAE
Climate	w/o Decomposition	1.120	0.859
	w/o TS-Text CL	1.184	0.888
	ETA	1.092	0.848
Energy	w/o Decomposition	0.254	0.368
	w/o TS-Text CL	0.250	0.363
	ETA	0.232	0.350
SocialGood	w/o Decomposition	0.892	0.440
	w/o TS-Text CL	0.944	0.475
	ETA	0.841	0.410

C.2 COMPARISON WITH PARAMETER-MATCHED ALTERNATIVES

we use gated-residual, cross-attention and FiLM for representation alignment and compare with ETA. The results are in Table 11. From these results, it is clear that methods like gated-residual and FiLM and cross-attention have higher MSE and MAE than ETA. Which means the methods struggle to effectively align the two highly distinct representation spaces of time series and text.

935
936
937
938
939
940
941
942
943
944
945
946
947
948
949
950
951
952
953
954
955
956
957
958
959
960
961
962
963
964
965
966
967
968
969
970
971
972
973
974
975
976
977
978
979
980
981
982
983
984
985
986
987
988
989
Table 11: **Ablation Study on Temporal Alignment Methods**

Dataset	Method	MSE	MAE
Climate	Gated-Residual	1.230	0.912
	Cross-Attention	1.202	0.893
	FiLM	1.211	0.897
	ETA	1.092	0.848
Energy	Gated-Residual	0.248	0.360
	Cross-Attention	0.254	0.369
	FiLM	0.252	0.367
	ETA	0.232	0.350
SocialGood	Gated-Residual	0.893	0.431
	Cross-Attention	0.887	0.427
	FiLM	0.894	0.431
	ETA	0.841	0.410

D ADAPTIVE FREQUENCY FUSION DESIGN DESCRIPTION

D.1 WHY CHOOSE LEARNABLE WEIGHTS INSTEAD OF LINEAR METHODS

Non-linear methods always have better fit ability. But we use 6 learnable parameter in stead of most non-linear method here for following reason. We need the Event-driven branch to forecast unseen patterns that cannot be learned from historical time series data and correct the numerical prediction. The unseen patterns always cause distribution shift. And we visualized the OT values of these datasets as shown in the Figure 8. We observe obvious distribution shifts between the training data and the test data. Therefore, non-linear methods may overfit the patterns learned from the training data and generalize poorly on the test data. In contrast, AFF uses only 6 parameters and aims to reflect the influence of text on time series, which generalizes better. We compare the results and provide them in the table below. The results in Table 12 show our AFF performs better than the non-linear methods, which support our analysis.

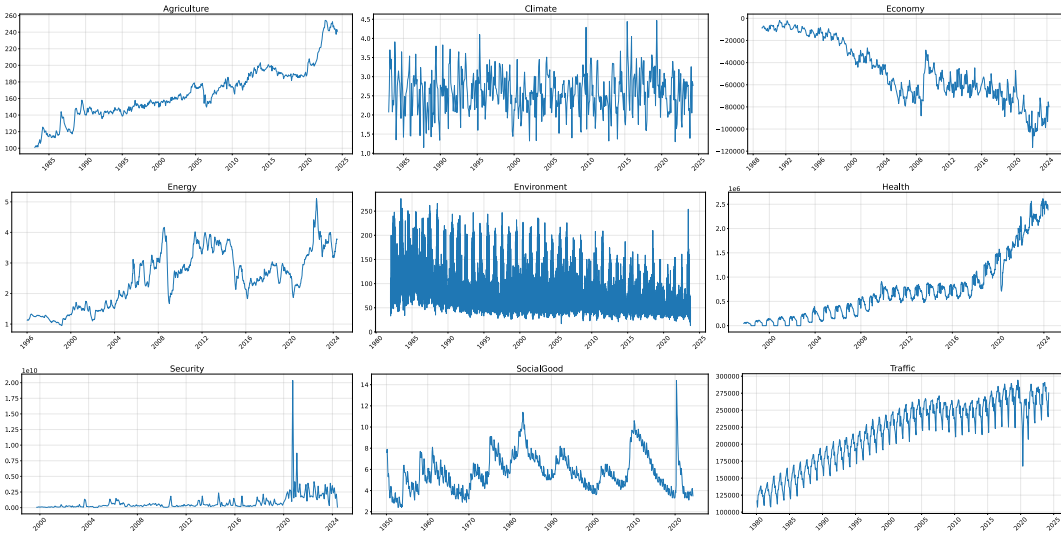


Figure 8: The visualization of the datasets

D.2 EVENT AND NON-EVENT PART ANALYSIS

To distinguish the event part and the non-event part in the data, we visualized the test datasets of Energy and SocialGood dataset and visually identified event segments (sudden shifts) and non-

990
991
992
993
994
995
996
997
998
999
1000
1001
1002
1003
1004
1005
1006
1007
1008
1009
1010
1011
1012
1013
1014
1015
1016
1017
1018
1019
1020
1021
1022
1023
1024
1025
1026
1027
1028
1029
1030
1031
1032
1033
1034
1035
1036
1037
1038
1039
1040
1041
1042
1043
1044
Table 12: Performance Comparison of Fusion Methods on Multiple Datasets

Dataset	Fusion Method	MSE	MAE
Climate	MLP	1.228	0.875
	Cross-Attention	1.768	1.055
	AFF	1.078	0.840
Energy	MLP	0.685	0.591
	Cross-Attention	0.430	0.502
	AFF	0.222	0.343
SocialGood	MLP	1.514	0.806
	Cross-Attention	1.459	0.842
	AFF	0.804	0.389

event segments (stable periods) in the test sets. Subsequently, we computed the MSE and MAE of the predictions of the two periods from two branches (the event-driven branch and the numerical branch), as well as the fused final prediction, in comparison with the ground truth. The results are presented in the Table 13.

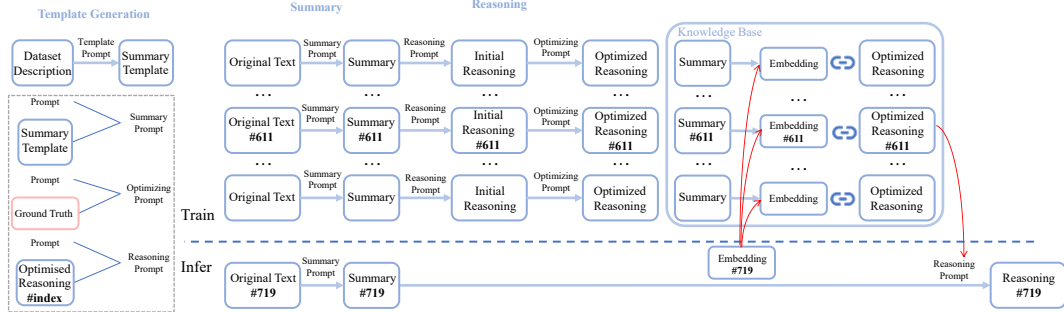
Upon analyzing these results, we observed that during the event period, the event-driven branch performs better than numerical predictions, and during the non-event period, numerical prediction is better. During the event period, the fusion method outperforms the numerical method, and during the non-event period, the fusion method is better than the event-driven method. This means the two predictions are complementary. For both the event part and the non-event part, the fusion method is better than both the event-driven and numerical prediction methods in some cases. For 'Overall', the fusion prediction is always better than the others, which is what we want. This can serve as proof that event-driven reasoning brings greater benefits to the event-related part than the harm to the non-event part, and ultimately leads to a better result.

Table 13: Prediction Performance Breakdown in Event and Non-Event Periods

Period	Branch	Energy		SocialGood	
		MSE	MAE	MSE	MAE
Event Part	Event-driven Branch	0.402	0.450	3.080	0.979
	Numerical Branch	0.443	0.523	3.339	1.022
	Fusion Result	0.362	0.460	3.084	0.969
Non-Event Part	Event-driven Branch	0.266	0.362	0.116	0.270
	Numerical Branch	0.105	0.257	0.068	0.208
	Fusion Result	0.125	0.269	0.066	0.205
Overall	Event-driven Branch	0.314	0.391	0.832	0.441
	Numerical Branch	0.244	0.360	0.861	0.405
	Fusion Result	0.222	0.343	0.804	0.389

Table 14: Pearson Correlation of Frequency Components (SocialGood)

Pred Length	Comparison	High Freq	Low Freq
8	Event-driven vs Ground Truth	0.155412	0.497763
	Numerical vs Ground Truth	0.423805	0.458464
10	Event-driven vs Ground Truth	0.265945	0.402431
	Numerical vs Ground Truth	0.349408	0.381150
12	Event-driven vs Ground Truth	0.273838	0.466686
	Numerical vs Ground Truth	0.310766	0.436835

1045
1046
1047
1048
1049
1050
1051 E LLM GENERATION EXAMPLES FOR EVENT-DRIVEN PREDICTION1052
1053
1054
1055
1056
1057
1058
1059
1060 This section demonstrates the complete event-driven prediction pipeline through concrete examples
from our US unemployment rate forecasting experiments.1061
1062 Figure 9: Illustration of the LLM generation pipeline for event-driven prediction. The process flows
1063 from template generation through summarization to reasoning, enhanced by Historical In-Context
1064 Learning that provides error-informed examples as guidance for improved forecasting accuracy.1065
1066 E.1 DATASET TEMPLATE GENERATION
10671068 • **Prompt Template:**1069
1070
1071
1072
1073
1074

```
prompt = f"""You are a professional data scientist. Based on the first 10 records
{sample data pairs} and dataset description{dataset description}, generate a
summary template for OT value prediction with domain knowledge..."""
```

1075
1076 • **Generated Template (SocialGood Dataset):**1077
1078
1079
1080
1081
1082
1083
1084
1085
1086
1087
1088
1089
1090
1091
1092
1093
1094

```
{
    "Dataset Name": "Unemployment Rate OT Value Prediction Dataset",
    "Description": "Monthly unemployment statistics for the United States, disaggregated by race",
    "Data Type": "Time series data, text data",
    "Data Source": "U.S. Department of Labor, BLS",
    "Time Span": "1954 to present (monthly data), 1994 to present (annual reports), 1979 to 1980 (text data)",
    "Sampling Method": "Comprehensive data from official reports",
    "OT Value": "Unemployment Rate",
    "Significance": "Indicator of economic health and societal impact",
    "Possible Relationships": {
        "Temporal": "OT value changes over time",
        "Spatial": "Racial disparities in unemployment rates",
        "Causal": "Economic policies and demographic changes"
    },
    "Features for Prediction": {
        "Trends in Time Series": "Historical trends and seasonality",
        "Key Information in Text Content": "Economic indicators and policy changes",
        "Domain Knowledge": "Economics, labor markets, and demographic trends"
    },
    "Trend Analysis for Prediction": {
        "Short-Term Trends": "Recent fluctuations in the OT value",
        "Long-Term Trends": "Historical patterns and future projections",
        "Cyclical Trends": "Business cycle impact",
        "Demographic Trends": "Changes in population size and structure"
    }
}
```

1095
1096
1097 E.2 SUMMARY GENERATION
10981099 • **Prompt Template:**

```

1100
1101
1102
1103
1104
1105
1106
1107
1108
1109
1110
1111
1112
1113
1114
1115
1116
1117
1118
1119
1120
1121
1122
1123
1124
1125
1126
1127
1128
1129
1130
1131
1132
1133
1134
1135
1136
1137
1138
1139
1140
1141
1142
1143
1144
1145
1146
1147
1148
1149
1150
1151
1152
1153
1154

```

```

base_prompt = f"""You are a professional data scientist analyzing a specific time
window of data.
TASK
Generate a NEW and UNIQUE analytical summary for this specific time window
({start_time}) to ({end_time}) of the {dataset_name} dataset.
REFERENCE INFORMATION (DO NOT COPY-ONLY FOR CONTEXT)
{dataset_description}
REQUIRED OUTPUT STRUCTURE
Your output must follow this JSON structure, but with YOUR OWN analysis:
{template}
INPUT DATA TO ANALYZE
Time Series Data for this window:
{time_series_str}
Text Data for this window:
{texts_str}
"""

instructions = """
IMPORTANT INSTRUCTIONS:
1. Your output must be a valid JSON object only.
2. DO NOT COPY descriptions from the reference information!
3. CREATE NEW analysis specific to THIS time window data.
4. Focus on the trends, patterns, and insights from THIS specific time period.
5. Your analysis should reflect what's happening in the provided time series and
text data.
Respond with ONLY the requested JSON object."""

```

- **Training Window #611 Summary (Dec 2000-Jul 2001):**

```

1126
1127
1128
1129
1130
1131
1132
1133
1134
1135
1136
1137
1138
1139
1140
1141
1142
1143
1144
1145
1146
1147
1148
1149
1150
1151
1152
1153
1154

```

```

{
    "Dataset Name": "US Racial Unemployment OT Value Prediction Dataset",
    "Description": "Monthly unemployment statistics for the United States,
disaggregated by racial groups",
    "Data Type": "Time series data, text data",
    "Data Source": "U.S. Bureau of Labor Statistics (BLS)",
    "Time Span": "August 2001 to March 2002 (monthly data)",
    "Sampling Method": "Comprehensive data from official employment reports",
    "OT Value": "Average Unemployment Rate Across All Groups",
    "Significance": "Indicator of workforce dynamics and policy implications",
    "Possible Relationships": {
        "Temporal": "Seasonal fluctuations influenced by macroeconomic factors",
        "Spatial": "Regional differences impacted by industry composition and
skill requirements",
        "Causal": "GDP changes, monetary policy, and post-9/11 economic impacts"
    },
    "Features for Prediction": {
        "Trends in Time Series": "Historical seasonality and unemployment
patterns",
        "Key Information in Text Content": "Macroeconomic indicators and industry
composition changes",
        "Domain Knowledge": "Labor economics, racial demographics, and economic
shocks"
    },
    "Trend Analysis for Prediction": {
        "Short-Term Trends": "Overall downward trend during specified period (90%
confidence)",
        "Long-Term Trends": "Historical unemployment patterns across racial
groups",
        "Cyclical Trends": "Increased variability post-9/11 attacks (80%
confidence)",
        "Demographic Trends": "Variations in unemployment rates by racial group"
    },
    "OT": "[4.9, 4.7, 5.0, 5.3, 5.4, 6.3, 6.1, 6.1]"
}

```

- **Test Window #719 Summary (Dec 2009-Jul 2010):**

```
1155
1156
1157 {
1158     "Dataset Name": "US Unemployment Trend Analysis",
1159     "Description": "Analyzing the trend of unemployment rate in the US from Dec
1160     2009 to Jul 2010.",
1161     "Data Type": "Mixed time series and text data",
1162     "Data Source": "Bureau of Labor Statistics (BLS)",
1163     "Time Span": "Dec 2009-Jul 2010",
1164     "Sampling Method": "Regular reporting from multiple sources including
1165     government agencies and academic institutions",
1166     "OT Value": "US Unemployment Rate",
1167     "Significance": "Indicates the overall health of the US economy and potential
1168     impact on society",
1169     "Possible Relationships": {
1170         "Temporal": "Seasonal fluctuations and historical trends influencing
1171         current unemployment rate",
1172         "Spatial": "Regional differences in unemployment rates indicating localized
1173         economic conditions"
1174     },
1175     "Features for Prediction": {
1176         "Trends in Time Series": "Identifying short-term and medium-term trends
1177         based on past performance",
1178         "Key Information in Text Content": "Understanding the underlying causes of
1179         unemployment through contextual analysis",
1180         "Domain Knowledge": "Familiarity with macroeconomic factors affecting
1181         employment rates"
1182     },
1183     "Trend Analysis for Prediction": {
1184         "Short-Term Trends": "Notable decline in unemployment rate after reaching
1185         peak in Mar-Apr 2010 followed by slight rebound before stabilizing near initial
1186         values",
1187         "Long-Term Trends": "Gradual upward movement since Sep-Dec 2009 indicates
1188         stabilization of workforce participation",
1189         "Cyclical Trends": "Influence of business cycles contributing to periods of
1190         accelerated hiring and layoffs throughout observation window",
1191         "Demographic Trends": "Shift toward part-time/full-time employment
1192         distributions possibly linked to seasonal variations in service sector
1193         activities"
1194     },
1195     "OT": "[9.7, 10.6, 10.4, 10.2, 9.5, 9.3, 9.6, 9.7]"
1196 }
1197 }
```

E.3 INITIAL PREDICTION AND CORRECTED REASONING

- **Prompt Template:**

```
1193 prompt = f"""<s>[INST] You are a quantitative analyst specializing in multimodal
1194 time series forecasting.
1195 - Window Length: {window_size}
1196 - Prediction Length: {prediction_length}
1197 TASK: Predict next {prediction_length} values for {dataset_name} using textual
1198 summary and window data.
1199 ANALYSIS:
1200 1. Textual Intelligence: Extract insights from summary
1201 2. Numerical Patterns: Identify trends and cycles
1202 3. Domain Knowledge: Apply sector understanding
1203 EXAMPLE: {fixed_example}
1204 SUMMARY: {summary}
1205 OUTPUT: JSON format exactly:
1206     ``json
1207         "Prediction": "",
1208         "Reasoning": "Brief explanation of key factors driving the prediction"
1209     ...
1210 
```

- **Initial Prediction for Window #611:**

```
1210
1211
1212 {
1213     "Summary..."
1214     "predicted_values": [6.0, 5.8, 5.6, 5.5, 5.4, 5.3, 5.2, 5.1, 5.0, 4.9, 4.8,
1215     4.7],
1216     "actual_values": [5.7, 5.5, 6.0, 5.9, 5.7, 5.4, 5.3, 5.6, 5.7, 6.5, 6.4,
1217     6.2],
1218     "original_reasoning": "The prediction reflects a gradual downward trend in
1219     unemployment rates, consistent with the 90% confidence level for an overall
1220     decline. The initial higher values account for post-9/11 variability (80%
1221     confidence), followed by stabilization as macroeconomic recovery takes effect.
1222     Seasonal adjustments and improving economic indicators suggest a return to
1223     pre-shock levels over the 12-month horizon.",
1224     "ot_values": "[4.9, 4.7, 5.0, 5.3, 5.4, 6.3, 6.1, 6.1]"
1225 }
```

- **Prompt Template:**

```
1223 prompt = f"""<s>[INST] You are an expert analyst tasked with improving prediction
1224 reasoning by learning from actual outcomes.
1225 DATASET: dataset_name
1226 WINDOW SUMMARY: {summary}
1227 PREDICTION ANALYSIS:
1228     - Original Prediction: {Original_Prediction}
1229     - Actual Values: actual_str
1230 ORIGINAL REASONING: {original_reasoning}
1231 TASK: Rewrite the reasoning process by incorporating insights from the actual
1232 outcomes. Focus on:
1233 1. Pattern Recognition: What patterns in the actual data were missed or correctly
1234 identified?
1235 2. Factor Analysis: Which factors had stronger/weaker impact than initially
1236 predicted?
1237 3. Trend Understanding: How did the actual trend differ from expectations?
1238 4. Domain Insights: What domain-specific knowledge can be extracted from this
1239 comparison?
1240 OUTPUT: JSON format exactly:
1241     '''json
1242     {
1243         "Improved_Reasoning": "Comprehensive analysis incorporating actual outcomes
1244 and improved understanding",
1245         "Key_Insights": "3-5 bullet points of key learnings from this prediction vs
1246 reality comparison",
1247         "Prediction_Factors": "Updated understanding of the most important prediction
1248 factors"
1249     }..
1250     [/INST]</s>"""
```

- **Corrected Reasoning:**

```
1245
1246    {
1247        "Summary..."
1248        "original_reasoning..."
1249        "improved_reasoning": "The original prediction anticipated a gradual
1250        downward trend in unemployment rates, influenced by post-9/11 variability and
1251        macroeconomic recovery. However, the actual data revealed a more complex pattern,
1252        with fluctuations that did not align with the expected stabilization. Notably,
1253        the actual unemployment rates showed heightened variability and an upward trend
1254        toward the end of the period, contrary to the predicted decline. This discrepancy
1255        suggests that the initial model underestimated the lingering effects of the 9/11
1256        attacks and overestimated the speed of economic recovery. Incorporating these
1257        insights, future predictions should account for prolonged external shocks and
1258        their nonlinear impacts on unemployment trends.",
1259        "key_insights": [
1260            "The actual data exhibited more variability and an upward trend toward the
1261            end of the period, contrary to the predicted gradual decline.",
1262            "The lingering effects of the 9/11 attacks had a more prolonged and severe
1263            impact on unemployment rates than initially anticipated.",
1264            "Macroeconomic recovery was slower than predicted, highlighting the need
1265            for more conservative estimates in post-crisis scenarios.",
1266            "Seasonal adjustments and industry composition changes may have been less
1267            influential than external shocks in this period."
1268        ],
1269        "prediction_factors": "Updated understanding emphasizes the importance of:
1270        1) accounting for prolonged external shocks (e.g., geopolitical events), 2)
1271        adjusting recovery timelines based on real-time economic indicators, and 3)
1272        incorporating nonlinear impacts of macroeconomic factors on unemployment rates."
1273    }
```

1265 E.4 HIC-GUIDED PREDICTION (TEST PHASE)
1266

1267 • RAG Retrieval for Window #719:

```

1268 {
1269     "similar_example_window": 611,
1270     "similarity_score": 0.8278101086616516,
1271     "retrieval_method": "Summary_Based_RAG_EMBEDDING"
1272 }
```

1273 • Prompt Template:

```

1274 prompt = f"""<s>[INST] You are a quantitative analyst specializing in multimodal
1275 time series forecasting.
1276 - Window Length: {window_size}
1277 - Prediction Length: {prediction_length}
1278 TASK: Predict next {prediction_length} values for {dataset_name} using textual
1279 summary and window data.
1280 ANALYSIS:
1281 1. Textual Intelligence: Extract insights from summary
1282 2. Numerical Patterns: Identify trends and cycles
1283 3. Domain Knowledge: Apply sector understanding
1284 EXAMPLE: {retrieved_example}
1285 SUMMARY: {summary}
1286 OUTPUT: JSON format exactly:
1287     '''json
1288         "Prediction": "",
1289         "Reasoning": "Brief explanation of key factors driving the prediction"
1290     '''
1291     [/INST]</s>"""
1292
1293
1294
1295
1296
```

1297 • Generated Prediction with HIC:

```

1298 {
1299     "prediction": [9.8, 9.9, 10.1, 10.2, 10.0, 9.8,
1300         9.7, 9.6, 9.5, 9.4, 9.3, 9.2],
1301     "reasoning": "Analysis suggests gradual stabilization following
1302         pattern from similar historical window. Incorporates insights
1303         about underestimating short-term fluctuations. Prediction reflects
1304         balanced view considering cyclical nature and potential volatility
1305         learned from Window #611's error patterns."
1306 }
```

1297 E.5 ANALYSIS OF EVENT-DRIVEN DESIGN
1298

1299 The above examples vividly illustrate how our event-driven prediction approach transforms the chal-
1300 lenge of multimodal time series forecasting into a continuous learning process. Consider the journey
1301 of Window #611 during the 2000-2001 economic downturn: while the initial prediction correctly
1302 identified an upward trend in unemployment, it projected a smooth, gradual increase from 4.8%
1303 to 5.9%. Reality proved far more turbulent—unemployment spiked sharply to 6.3% following the
1304 September 11 attacks before showing unexpected resilience in recovery. This discrepancy between
1305 prediction and reality became a valuable learning opportunity. Through error analysis, the system
1306 discovered that external shocks create discontinuities that pure trend analysis cannot capture, lead-
1307 ing to a fundamental recalibration of prediction weights: historical trends were reduced from 40% to
1308 30% importance while economic shock factors increased from 20% to 35%. This learned knowledge
1309 proves its worth when the system encounters Window #719 during the 2009-2010 financial crisis
1310 period. Through embedding similarity analysis, the system recognizes a kindred pattern between
1311 these two economic downturns, achieving a similarity score of 0.8278. This recognition triggers the
1312 retrieval of Window #611's hard-won insights about volatility and recovery patterns. Rather than re-
1313 peating the mistake of over-smooth predictions, the forecast for Window #719 now incorporates the
1314 understanding that crisis periods exhibit both sharp fluctuations and surprising stabilization mech-
1315 anisms. The resulting prediction balances the observed stabilization trend with awareness of potential
1316 volatility, producing a more nuanced trajectory from 9.8% gradually declining to 9.2%. What makes
1317 this approach particularly compelling is how it mirrors human expert reasoning in economic fore-
1318 casting. Just as economists draw parallels between historical crises to inform current predictions,
1319 our HIC systematically captures and transfers these insights across similar economic conditions.
The system essentially builds a memory of how past events translated into numerical outcomes,
creating a bridge between the rich semantic information in news reports, policy announcements,

1320 and economic analyses, and the quantitative requirements of time series forecasting. This design
 1321 achieves what pure numerical models struggle with—understanding that a phrase like “unprece-
 1322 dented economic shock” carries specific implications for unemployment volatility based on histori-
 1323 cal precedent—while avoiding the computational expense of fine-tuning large language models for
 1324 each specific domain.

1325 F SUPPLEMENTARY

1326 Table 15: Ablation study on different LLMs

1330 LLM	1331 Energy		1332 Social Good	
	1333 MSE	1334 MAE	1335 MSE	1336 MAE
1337 DeepSeek	0.222	0.343	0.804	0.389
1338 Zhipu	0.229	0.337	0.829	0.411
1339 Qwen	0.226	0.341	0.773	0.427

1340 We also attempted to conduct experiments using different models with various parameter quantities.
 1341 The experimental results showed in Table 15 indicated that under our method, LLMs could all
 1342 provide excellent assistance for time series forecasting and outperform other methods.

1343 G COMPREHENSIVE EXPERIMENTAL RESULTS

1344 This appendix provides comprehensive experimental results for all methods across different predic-
 1345 tion horizons on 10 multimodal time series datasets.

1346
 1347
 1348
 1349
 1350
 1351
 1352
 1353
 1354
 1355
 1356
 1357
 1358
 1359
 1360
 1361
 1362
 1363
 1364
 1365
 1366
 1367
 1368
 1369
 1370
 1371
 1372
 1373
 1374

1375
 1376
 1377
 1378
 1379
 1380
 1381
 1382
 1383
 1384
 1385
 1386
 1387
 1388
 1389
 1390
 1391
 1392
 1393
 1394
 1395
 1396
 1397
 1398
 1399
 1400
 1401
 1402
 1403
 1404
 1405
 1406
 1407
 1408
 1409
 1410
 1411
 1412
 1413
 1414
 1415
 1416
 1417
 1418
 1419
 1420
 1421
 1422
 1423
 1424
 1425
 1426
 1427
 1428
 1429

Table 16: Model Performance Comparison Across Different Categories

Category	TS-only										Text-enhanced										Multimodal													
	numerical branch					iTransformer					Raft					iTransformer*					PatchTST*		Raft*		GPT4TS		GPT4MTS		TAT5		TimeVLM		CALF	
	Models	MSE	MAE	MSE	MAE	MSE	MAE	MSE	MAE	MSE	MSE	MAE	MSE	MAE	MSE	MAE	MSE	MAE	MSE	MAE	MSE	MAE	MSE	MAE	MSE	MAE	MSE	MAE						
Agriculture	6	0.131	0.245	0.146	0.256	0.128	0.254	0.151	0.254	0.154	0.265	0.146	0.263	0.157	0.282	0.135	0.242	0.161	0.257	0.140	0.251	0.143	0.245	0.142	0.250	0.142	0.250	0.142	0.250					
	8	0.182	0.286	0.188	0.287	0.200	0.296	0.197	0.287	0.194	0.296	0.195	0.290	0.189	0.310	0.237	0.344	0.198	0.284	0.207	0.288	0.215	0.287	0.215	0.285	0.215	0.285	0.215	0.285					
	10	0.235	0.319	0.221	0.317	0.254	0.320	0.252	0.320	0.254	0.326	0.254	0.320	0.254	0.326	0.254	0.326	0.254	0.328	0.254	0.320	0.244	0.320	0.244	0.320	0.244	0.320	0.244	0.320					
	12	0.288	0.355	0.301	0.356	0.300	0.352	0.309	0.351	0.301	0.383	0.305	0.352	0.338	0.369	0.326	0.379	0.291	0.338	0.301	0.342	0.290	0.350	0.322	0.359	0.314	0.355	0.314	0.355					
Climate	avg	0.209	0.302	0.214	0.304	0.220	0.308	0.228	0.303	0.226	0.229	0.310	0.232	0.316	0.246	0.333	0.220	0.294	0.225	0.298	0.215	0.301	0.238	0.303	0.250	0.315	0.250	0.315						
	6	1.071	0.840	1.090	0.847	1.111	0.860	1.197	0.896	1.298	0.925	1.117	0.857	1.206	0.898	1.292	0.924	1.207	0.901	1.199	0.895	1.194	0.897	1.218	0.907	1.231	0.910	1.231	0.910					
	8	1.075	0.837	1.074	1.074	1.147	0.866	1.183	0.892	1.260	0.918	1.119	0.863	1.169	0.885	1.435	0.975	1.205	0.899	1.178	0.886	1.181	0.914	1.227	0.905	1.227	0.905	1.227	0.905					
	10	1.078	0.836	1.087	0.843	1.152	0.870	1.188	0.886	1.301	0.932	1.118	0.858	1.168	0.882	1.296	0.929	1.169	0.886	1.173	0.885	1.170	0.881	1.179	0.880	1.179	0.880	1.179	0.880					
Economy	12	1.088	0.845	1.118	0.861	1.131	0.877	1.168	0.877	1.295	0.930	1.115	0.855	1.171	0.881	1.345	0.947	1.171	0.883	1.152	0.876	1.179	0.885	1.203	0.896	1.177	0.883	1.177	0.883					
	avg	1.078	0.840	1.092	0.848	1.135	0.865	1.184	0.888	1.289	0.926	1.117	0.858	1.178	0.887	1.342	0.944	1.184	0.891	1.182	0.889	1.180	0.887	1.195	0.899	1.286	0.922	1.286	0.922					
	avg	0.201	0.353	0.203	0.358	0.222	0.378	0.210	0.363	0.265	0.411	0.213	0.367	0.219	0.370	0.275	0.420	0.217	0.371	0.208	0.363	0.215	0.368	0.229	0.384	0.207	0.357	0.207	0.357					
	12	0.091	0.218	0.101	0.225	0.121	0.258	0.107	0.235	0.123	0.255	0.124	0.231	0.124	0.271	0.105	0.232	0.116	0.242	0.111	0.244	0.105	0.232	0.114	0.224	0.114	0.224							
Energy	24	0.184	0.314	0.199	0.325	0.221	0.338	0.211	0.339	0.220	0.340	0.218	0.334	0.220	0.345	0.214	0.340	0.216	0.344	0.212	0.342	0.216	0.344	0.212	0.344	0.212	0.344	0.212	0.344					
	36	0.278	0.393	0.300	0.406	0.279	0.399	0.298	0.390	0.295	0.405	0.306	0.413	0.321	0.423	0.308	0.413	0.292	0.402	0.314	0.423	0.308	0.403	0.309	0.420	0.309	0.420	0.309	0.420					
	48	0.337	0.446	0.440	0.405	0.488	0.448	0.408	0.447	0.474	0.467	0.438	0.475	0.512	0.385	0.475	0.372	0.465	0.393	0.484	0.398	0.496	0.391	0.480	0.390	0.475	0.390	0.475						
	avg	0.222	0.341	0.232	0.350	0.269	0.382	0.250	0.363	0.254	0.367	0.265	0.383	0.253	0.365	0.261	0.386	0.260	0.376	0.262	0.380	0.255	0.368	0.260	0.374	0.255	0.365							
Environment	48	0.273	0.384	0.281	0.377	0.228	0.384	0.307	0.390	0.326	0.409	0.278	0.386	0.306	0.395	0.321	0.406	0.323	0.406	0.321	0.406	0.322	0.407	0.324	0.406	0.322	0.406	0.324	0.406					
	96	0.270	0.378	0.273	0.381	0.223	0.358	0.221	0.339	0.220	0.345	0.218	0.334	0.216	0.351	0.214	0.340	0.212	0.340	0.214	0.344	0.212	0.344	0.212	0.344	0.212	0.344	0.212	0.344					
	192	0.273	0.384	0.288	0.390	0.230	0.366	0.228	0.349	0.230	0.360	0.228	0.349	0.230	0.363	0.228	0.360	0.226	0.363	0.228	0.367	0.226	0.368	0.226	0.367	0.226	0.368	0.226	0.367					
	336	0.256	0.374	0.374	0.226	0.356	0.224	0.349	0.226	0.357	0.220	0.349	0.224	0.352	0.222	0.358	0.220	0.357	0.222	0.359	0.220	0.361	0.220	0.367	0.220	0.367	0.220	0.367						
Health	avg	0.268	0.380	0.322	0.376	0.274	0.386	0.317	0.395	0.339	0.343	0.423	0.278	0.390	0.318	0.397	0.337	0.347	0.322	0.333	0.340	0.319	0.396	0.320	0.387	0.320	0.387	0.320	0.387					
	12	0.898	0.596	0.926	0.612	1.261	0.746	1.006	0.650	1.062	0.650	0.896	1.231	0.728	0.866	1.280	0.760	1.312	0.766	0.854	0.629	0.985	0.658	0.899	0.612	1.198	0.727	0.964	0.699	1.198	0.727	0.964		
	24	1.210	0.707	1.275	0.729	1.476	0.816	1.403	0.799	1.773	0.963	1.936	1.025	1.524	1.026	1.724	1.026	1.722	0.972	1.721	0.973	1.721	1.027	1.759	1.027	1.759	1.027	1.759	1.027	1.759				
	48	1.249	0.802	1.459	0.810	1.780	1.615	1.871	1.787	2.075	1.615	2.075	1.721	1.910	1.721	2.075	1.721	1.910	1.721	2.075	1.721	1.910	1.721	2.075	1.721	2.075	1.721	2.075	1.721	2.075				
Social Good	avg	0.675	0.340	0.704	0.344	0.780	0.376	0.724	0.362	0.796	0.375	0.763	0.370	0.750	0.376	0.763	0.370	0.750	0.376	0.763	0.370	0.750	0.370	0.750	0.370	0.750	0.370	0.750						
	8	0.774	0.386	0.806	0.395	0.849	0.430	0.870	0.431	0.897	0.430	0.897	0.431	0.897	0.430	0.897	0.431	0.897	0.430	0.897	0.431	0.897	0.430	0.897	0.430	0.897	0.430	0.897						
	10	0.844	0.402	0.842	0.414	0.914	0.509	0.978	0.511	1.017	0.511	1.017	0.511	1.017	0.511	1.017	0.511	1.017	0.511	1.017	0.511	1.017	0.511	1.017	0.511	1.017	0.511	1.017						
	12	0.925	0.438	0.962	0.457	1.153	0.574	1.263	0.643	1.151	0.553	1.285	0.653	1.050	1.050	0.477	0.477	1.141	0.550	1.167	0.608	1.093	0.470	1.053	0.470	1.053	0.470	1.053						
Traffic	avg	0.169	0.232	0.172	0.232	0.184	0.238	0.176	0.234	0.184	0.238	0.184	0.234	0.184	0.238	0.184	0.234	0.184	0.238	0.184	0.234	0.184	0.238	0.184	0.234	0.184	0.234							
	6	0.155	0.227	0.160	0.233	0.168	0.235	0.160	0.228	0.170	0.234	0.168	0.232	0.168	0.232	0.168	0.232	0.168	0.232	0.168	0.232	0.168	0.232	0.168	0.232	0.168	0.232							
	8	0.167	0.231	0.170	0.236	0.173	0.237	0.171	0.237	0.174	0.237	0.173	0.237	0.172	0.																			